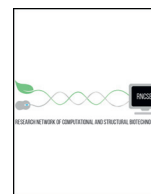




ELSEVIER



COMPUTATIONAL
AND STRUCTURAL
BIOTECHNOLOGY
JOURNAL

journal homepage: www.elsevier.com/locate/csbj

Discovery of novel quinazoline derivatives bearing semicarbazone moiety as potent EGFR kinase inhibitors

Yuanbiao Tu^{a,b,1}, Caolin Wang^{a,1}, Zunhua Yang^c, Bingbing Zhao^a, Luogen Lai^a, Qi Yang^a, Pengwu Zheng^{a,*}, Wufu Zhu^{a,*}

^a Jiangxi Provincial Key Laboratory of Drug Design and Evaluation, School of Pharmacy, Jiangxi Science & Technology Normal University, Nanchang 330013, PR China

^b Department of Biomedical Engineering, School of Engineering, China Pharmaceutical University, Nanjing 210009, PR China

^c College of Pharmacy, Jiangxi University of Traditional Chinese Medicine, Nanchang 330004, PR China

ARTICLE INFO

Article history:

Received 1 September 2018

Received in revised form 24 October 2018

Accepted 26 October 2018

Available online 30 October 2018

Keywords:

Quinazoline

Semicarbazone moiety

EGFR kinase inhibitors

Anti-tumor activity

Docking study

ABSTRACT

Aimed at discovering effective EGFR inhibitors, six series of quinazoline derivatives bearing a semicarbazone moiety were designed, synthesized and evaluated in different cancer cell lines (A549, HepG2, MCF-7 and PC-3). Most of the selected compounds showed remarkable cytotoxicity with IC₅₀ values reaching the nanomole range. Further, the inhibition efficacy of 11 compounds against EGFR kinases was tested, which demonstrated excellent IC₅₀ values in nanomolar level. Importantly, 2 compounds exhibited IC₅₀ values of 0.05 nM and 0.1 nM against wild type EGFR respectively, suggesting more potent activities than that of the positive control, Afatinib (4.0 nM). Excitingly, 2 compounds showed excellent enzyme inhibitory activity with 8.6 nM and 5.6 nM for double T790 M/L858R mutant EGFRs, which is almost the same as Afatinib (3.8 nM). Structure–activity relationships (SARs) analysis indicated that the type of small molecule amine in pyrrole moiety or the chain length of pyrrolamine moiety had no obvious impact on the inhibition efficacy of our synthesized compounds against cancer cells. In addition, results of cell cycle analysis indicated that the G2/M phase of A549 cells was efficiently arrested by the selected compounds. These preliminary results demonstrate that 2 compounds may be promising lead compound–targeting EGFR.

© 2018 The Authors. Published by Elsevier B.V. on behalf of Research Network of Computational and Structural Biotechnology. This is an open access article under the CC BY-NC-ND license (<http://creativecommons.org/licenses/by-nc-nd/4.0/>).

1. Introduction

Epidermal growth factor receptor (EGFR) is a transmembrane glycoprotein which combines with epidermal growth factor (EGF) and activates vital cellular processes including proliferation, differentiation, migration, apoptosis, and angiogenesis [1–3]. Abnormal expression of EGFR has been validated in various tumors such as gastric cancer, breast cancer and bladder cancer [4]. Therefore, it is highly attractive to develop EGFR inhibitors with enhanced efficacy and reduced toxicity.

Currently, various quinazoline derivatives have been developed as EGFR inhibitors with excellent anti-tumor activity, such as Gefitinib [5,6], Afatinib [7–9] and BMC201725-9o [10] (Fig. 1). Among these inhibitors, Gefitinib is the first molecularly targeted EGFR inhibitor against non-small cell lung cancer (NSCLC) with IC₅₀ of 27 nM [11]. In particular, Afatinib, a second-generation EGFR inhibitor, has a Michael acceptor that can covalently and irreversibly bind to the

receptor, thus exhibiting more potent anti-tumor activity (IC₅₀ value of 0.5 nM). It has been approved by the FDA for the therapy of metastatic NSCLC in 2013 [12]. However, the irreversible binding of Afatinib to target protein may cause certain side effects to normal tissues that also express EGFR. The third-generation EGFR inhibitor, AZD9291, exhibits stronger antitumor efficacy by circumventing drug resistance. However, the higher dose of AZD9291 (80 mg/day, Afatinib 40 mg/day) in clinic leads to serious side effects such as severe cardiotoxicity, rash and diarrhea [13,14]. Such toxicity may also be attributed to the irreversible receptor binding. A recent study exposed the occurrence of the tertiary point mutation C797 in 40% of the patients treated with AZD9291 [15], because the drug molecules to lose covalent interactions caused by the mutation, resulting in a decrease in inhibitory activity. Therefore, developing noncovalent inhibitors for EGFR attracted the researchers' attention [16,17]. It is highly attractive if the currently used inhibitors can be optimized to reversibly bind to receptor and reserve high potency.

Qin et al. and Zhai et al. reported some potent tumor inhibitors possessed semicarbazone moiety with imine-type functionality [18,19]. In our previous investigation of the compounds that non-covalently bind to EGFR, BMC201725-9o showed the strongest

* Corresponding author.

E-mail addresses: zhengpw@126.com (P. Zheng), zhuwf@jxstnu.edu.cn (W. Zhu).

¹ These authors contributed equally to this work.

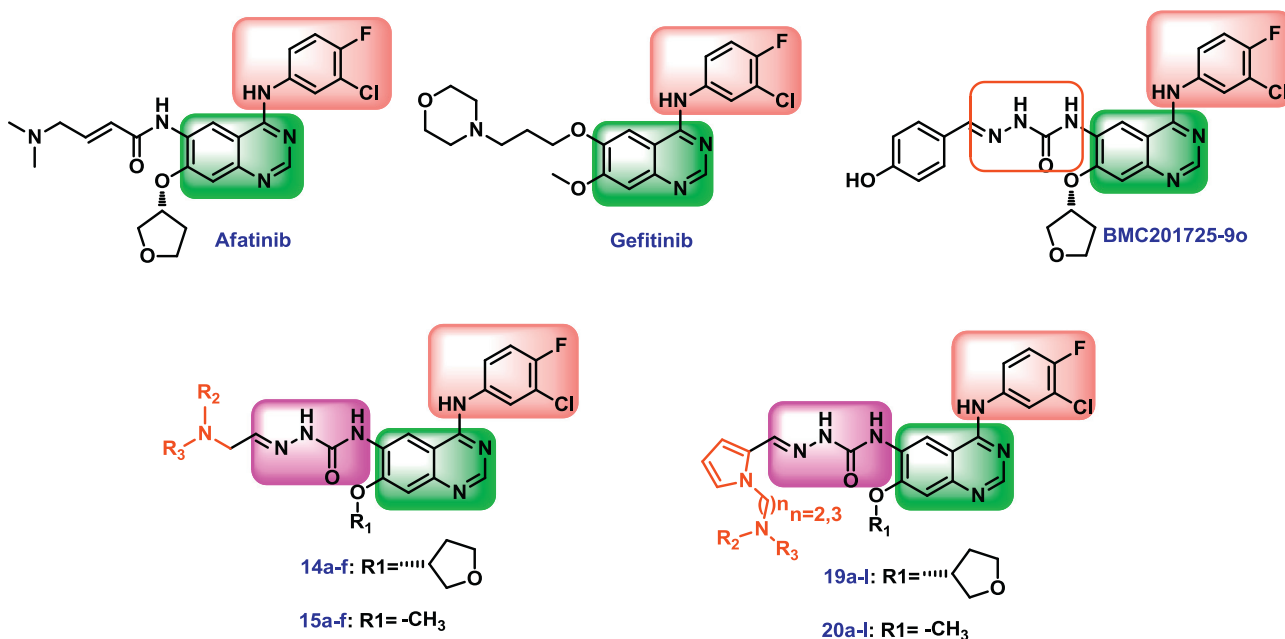


Fig. 1. Structures of EGFR inhibitors based on the quinazoline scaffold, BMC201725-9o and the designed compounds.

activity with the IC_{50} of 56 nM, because of the semicarbazone moiety [10]. However, the unsatisfactory solubility of this compound was the major limitation hindering its further development. In order to improve the solubility of BMC201725-9o, in this study, six series of quinazoline derivatives bearing a semicarbazone moiety were designed, synthesized. The design strategy is shown in Fig. 2. The anti-tumor activity of these compounds were evaluated in A549 (lung cancer), HepG2 (liver cancer), MCF-7 (breast cancer) and PC-3 (prostate cancer) cell lines. EGFR kinases assay was then performed for the selected compounds. Moreover, acridine orange (AO) single staining, cell cycle analysis and docking studies are presented in this paper as well.

2. Chemistry

The structures and preparation of target compounds **10a–e** and **11a–e** are described in Scheme 1.

The key intermediates **8a** and **8b** were synthesized from commercially available 2-amino-4-fluorobenzoic acid through eight steps which was reported in our previously research [10,20]. Finally, condensation of **8a** or **8b** with heterocyclic aldehydes in ethanol in the presence of a catalytic amount of glacial acetic acid yielded the target compounds **10a–e** and **11a–e**, respectively. The relative stereochemistry of the target compounds (**10a–e** and **11a–e**) was easily confirmed as *E* isomeric by the date of 1H NMR.

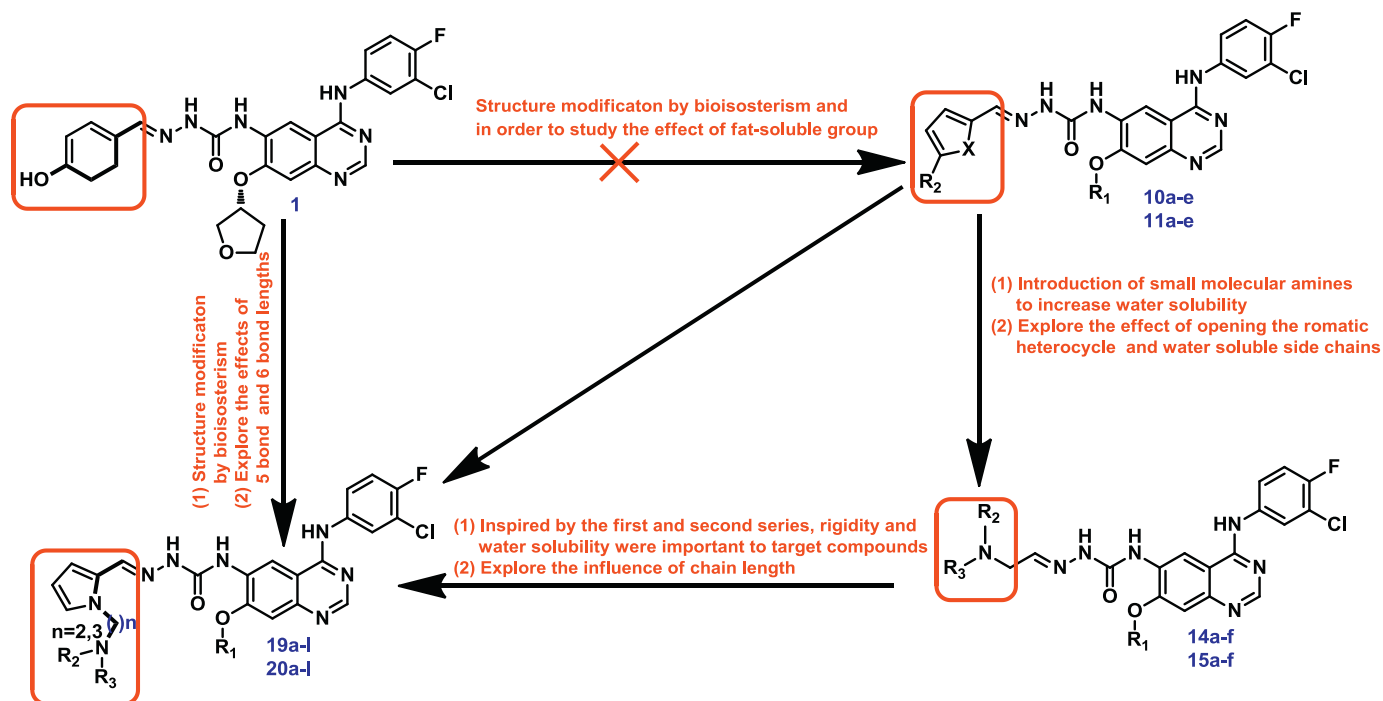
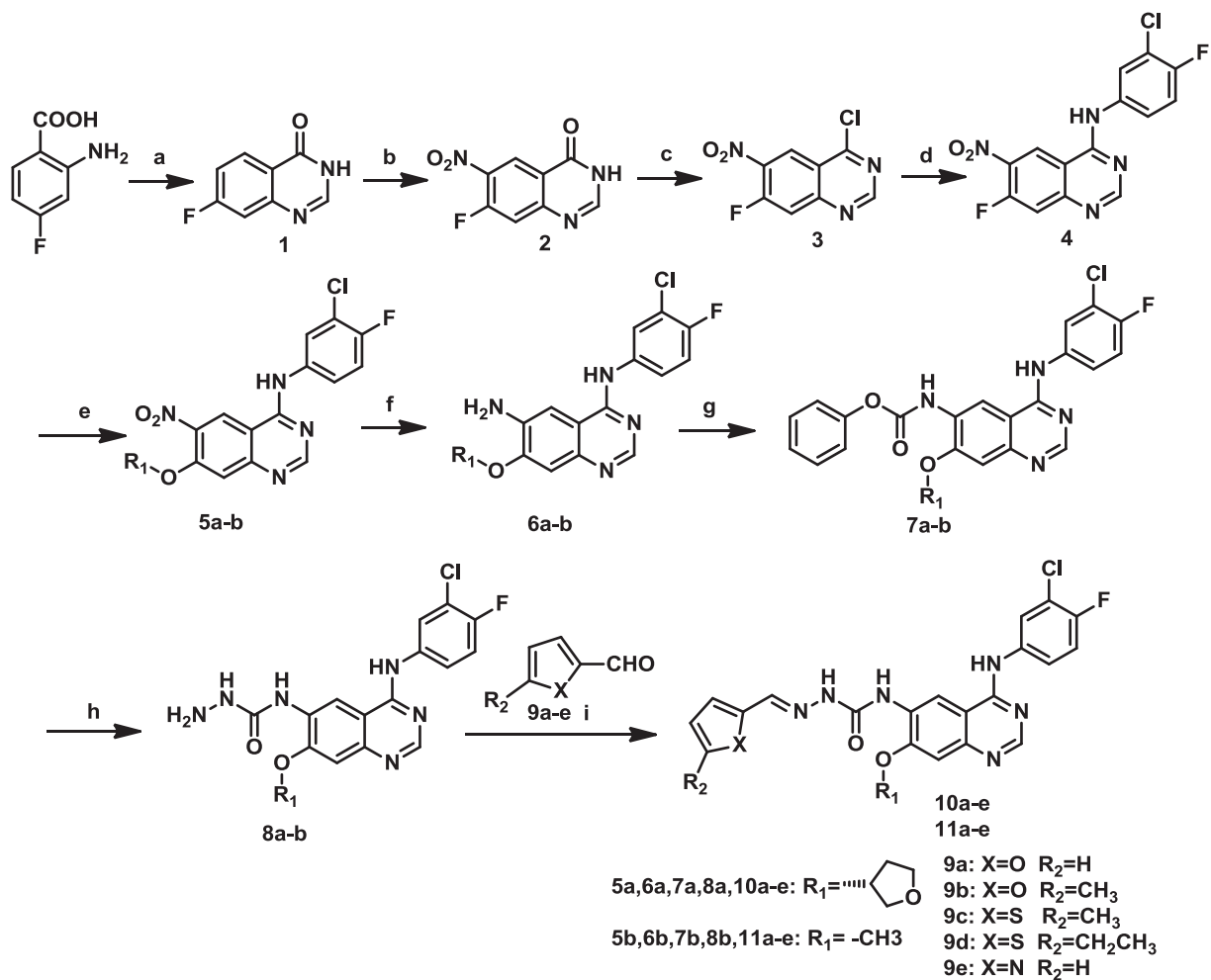
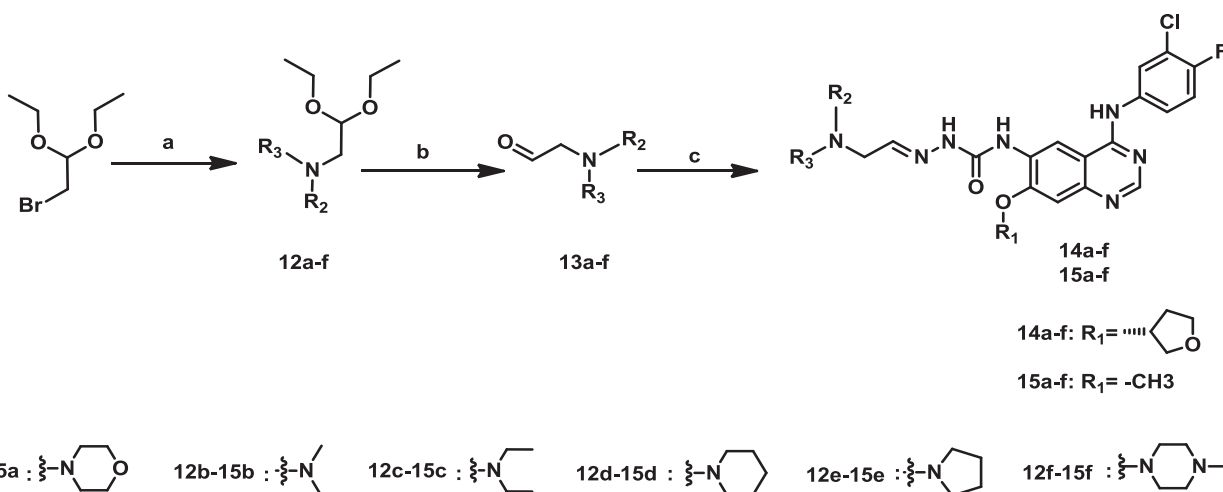


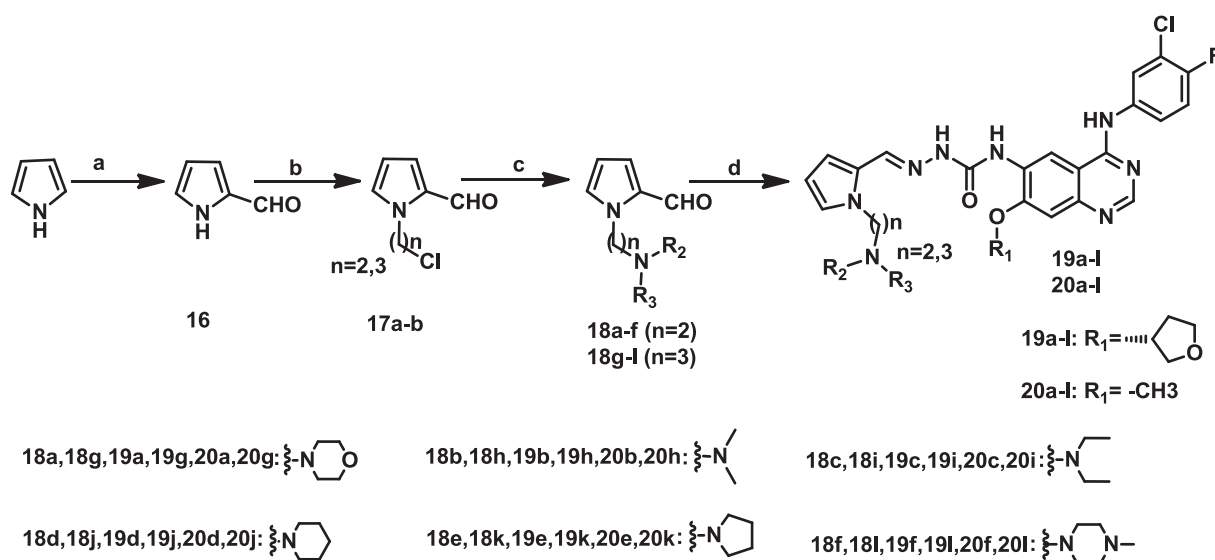
Fig. 2. Structures and design strategy of target compounds.



Scheme 1. Synthetic route of target compounds **10a-e** and **11a-e**. **Reagents and conditions:** (a) EtOH, Formamidinium acetate, 24 h; (b) Conc. H_2SO_4 , fuming HNO_3 , 2 h; (c) $SOCl_2$, DMF (Cat.), 4 h; (d) 3-Chloro-4-fluoroaniline, Isopropanol, Triethylamine, 1.5 h; (e) (S)-Tetrahydrofuran-3-ol, NaH (60%), THF, 3 h; CH_3OH , NaOH; (f) 80% Hydrazine monohydrate, $FeCl_3$, Activated Carbon, EtOH, 1 h; (g) Phenyl chloroformate, DIPEA, 1,4-Dioxane, 10 °C to rt., 1.5 h; (h) 80% Hydrazine monohydrate, 1,4-Dioxane, reflux; (i) Aldehyde, Acetic acid (Cat.), EtOH, reflux.



Scheme 2. Synthetic route of target compounds **14a-f** and **15a-f**. **Reagents and conditions:** (a) DMF, 100 °C, 2 h; (b) Conc. HCl, H_2O , 50 °C, 2 h; (c) **8a** or **8b**, EtOH, 80 °C, 2 h.



Scheme 3. Synthetic route of target compounds **19a-l** and **20a-l**. **Reagents and conditions:** (a) POCl₃, DMF, Dichloromethane, Potassium acetate; (b) NaH (60%), DMF, 1-Bromo-3-chloropropane or 1-Bromo-2-chloroethane; (c) DMF, Amine, 130 °C, 5 h; (d) **8a** or **8b**, DMSO, Conc. H₂SO₄ (Cat.), 70 °C, 5 h.

The structures and preparation of target compounds **14a-f** and **15a-f** are described in Scheme 2.

The intermediates **12a-f** were synthesized from 2-bromo-1,1-diethoxyethane via substitution reaction with small sized secondary amine, respectively. Following by deprotection, **13a-f** were obtained. Similarly, **14a-f** and **15a-f** were achieved from **13a-f** and **8a** or **8b** via condensation reaction.

The structures and preparation of target compounds **19a-l** and **20a-l** are described in Scheme 3.

The intermediate 1H-pyrrole-2-carbaldehyde (**16**) was synthesized from pyrrole, DMF and POCl₃ via Vilsmeier-Haack reaction [21]. Then the intermediates **16** was reacted with 1-chloro-2-bromoethane or 1-chloro-3-bromopropane in DMF in the present of NaH (60%) via substitution reaction to yielding the intermediate **17a-b**, which were then reacted with small molecule secondary amine via substitution reaction to obtain the compounds **18a-l**. Finally, condensation of **8a** or **8b** with pyrrole-2-carbaldehyde **18a-l** in DMSO in the presence of a catalytic amount of concentrated sulfuric acid yielded target compounds **19a-l** and **20a-l** respectively.

3. Results and discussion

3.1. Chemistry section

Six series of novel quinazoline derivatives bearing semicarbazone scaffolds (**10a-e**, **11a-e**, **14a-f**, **15a-f**, **19a-l** and **20a-l**) were designed and synthesized (Fig. 2). All target compounds were successfully synthesized starting from the key intermediate **8a** and **8b** according to the procedures in our previous research, and were characterized by mass spectrometry and ¹H NMR spectra. Some representative compounds were confirmed by ¹³C NMR spectra.

3.2. Biological evaluation

Taking Afatinib as the reference compound, the target compounds (**10a-e**, **11a-e**, **14a-f**, **15a-f**, **19a-l** and **20a-l**) were evaluated for the cytotoxicity against three or four cancer cell lines including A549, HepG2, MCF-7 and PC-3 by 3-(4,5-dimethylthiazolyl)-2, 5-diphenyltetrazolium bromide (MTT) cell proliferation assay. EGFR kinase inhibitory activity was further evaluated in the compounds (**14a**, **14b**, **14c**, **14e**, **14f**, **19a**, **19b**, **19i**, **19j**, **20b** and **20h**) in vitro, with Afatinib serving as reference compounds. The results of IC₅₀ values were

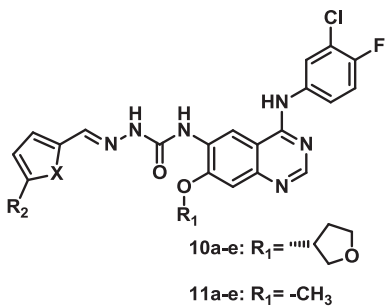
summarized in Tables 1, 2, 3, 4 and 5. Moreover, the concentration dependent activity of selected compounds (**14d** and **19b**) against four cancer cell lines (MCF-7, PC-3, A549 and HepG2) were demonstrated in Fig. 3. In addition, AO single staining was carried out in this study for the selected compounds (**14d** and **19b**) in A549 cell (Fig. 4), and cell cycle of the compound **14d** and **19b** were analyzed by flow cytometry (Fig. 5).

As illustrated in Table 1, eight of the synthesized compounds showed poor anti-proliferative activities against the three tested cancer cells except compounds **10e** and **11e** containing the pyrrole moiety. Interestingly, Compound **10e** exhibited the highest activity against A549, HepG2 and MCF-7 cell lines with the IC₅₀ values of 2.41 ± 0.32 μM, 0.59 ± 0.02 μM and 1.21 ± 0.19 μM respectively, which were slightly higher than that of afatinib (1.40 ± 0.83 μM, 1.33 ± 1.28 μM, 2.63 ± 1.06 μM).

In order to find inhibitors targeting L858R/T790 M, compounds **14a**, **14b**, **14c**, **14d**, and **14f** were further evaluated for the inhibitory activity against EGFR^{L858R/T790M} and EGFR^{WT} by using the well-established ELISA-based assay, and Afatinib was employed as positive control. As shown in Table 3, Among the compounds tested, all compounds showed single-digit nanomolar levels of wild-type kinase activity, which more active than the positive control Afatinib. Notably, Among them, compound **14d** was the best representative against wild-type kinase activity of EGFR (IC₅₀ 0.1 nM), which was higher than that of afatinib (IC₅₀ 4.0 nM). However, all compounds had slightly poorer inhibitory activity against the L858R/T790 M mutant than the positive control Afatinib.

Most of the pyrrole-substituted compounds exhibited excellent cytotoxic activities against the four cancer cell lines (Table 4). These compounds showed equal or even more potent activities than positive control Afatinib against one or more cell lines. The inhibitory activities of all the target compounds (**19a-l** and **20a-l**) against A549 cancer cell were superior to that of Afatinib. Except compounds **19a**, **19g**, **19h** and **20c**, the synthesized derivatives could more effectively inhibit the proliferation of HepG2 cancer cells than Afatinib. Remarkably, compounds **19b**, **20a**, **20d**, **20h**, **20k** and **20l** showed strong antitumor cell activities against HepG2 cell lines. Among them, the potential compounds **19b** well inhibited the growth of HepG2 cells with IC₅₀ values of 0.04 ± 0.01 μM, which was more active than Afatinib (1.16 ± 0.06 μM). Most of the target compounds **19a-l** and **20a-l** were equality active compared positive control Afatinib against the PC-3 cell lines. Notably, compounds

Table 1
Structures and activity of target compounds **10a–e** and **11a–e**.



Compd.	X	R ₂	IC ₅₀ ^a (μM)			LogD _{7.4} ^e
			A549	HepG2	MCF-7	
10a	O	—H	NA ^c	35.23 ± 1.53	33.42 ± 0.97	4.05
10b	O	—CH ₃	28.22 ± 1.34	33.25 ± 1.46	34.76 ± 1.01	4.25
10c	S	—CH ₃	28.35 ± 0.56	29.22 ± 1.43	26.12 ± 1.33	5.55
10d	S	—CH ₂ CH ₃	34.23 ± 0.31	36.20 ± 1.78	ND ^d	6.01
10e	N	—H	2.41 ± 0.32	0.59 ± 0.02	1.21 ± 0.19	3.99
11a	O	—H	26.23 ± 1.23	29.69 ± 1.86	ND ^d	4.15
11b	O	—CH ₃	28.22 ± 1.34	30.21 ± 1.16	35.16 ± 0.81	4.35
11c	S	—CH ₃	29.33 ± 0.36	27.42 ± 1.03	28.12 ± 1.13	5.65
11d	S	—CH ₂ CH ₃	35.28 ± 0.42	35.23 ± 1.08	ND ^d	6.09
11e	N	—H	8.41 ± 0.76	9.18 ± 1.05	9.31 ± 1.76	4.09
Afatinib^b	—	—	6.34 ± 0.01	1.16 ± 0.06	1.09 ± 0.01	2.34

^a Values are presented as the mean ± SD in two independent experiments.

^b Used as a positive control.

^c NA: not active.

^d ND: Not determined.

^e The result is predicted by <https://chemaxon.com/#/calculation>.

20 g and **20 h** exhibited superior inhibitory activity with IC₅₀ values of 0.05 ± 0.01 μM and 0.03 ± 0.01 μM, which were more active than Afatinib (1.13 ± 0.05 μM), respectively.

The anti-EGFR kinase activity of the selected compounds (**19a**, **19b**, **19i**, **19j**, **20b** and **20h**) was further evaluated. As shown in Table 5, the six selected compounds exerted comparable potency against wild type EGFR kinase than Afatinib. In particular, compound **19b** achieved IC₅₀ value of 0.05 nM, which was more active than Afatinib (0.5 nM). Furthermore, the IC₅₀ values of compounds **19b** against T790M/L858R mutant EGFRs is 5.6 nM, which is at same level as Afatinib (3.8 nM).

3.3. Concentration-dependent assay

In order to investigate the influence of concentration on cytotoxicity, MTT assay was performed using five sequential concentrations of Afatinib and selected compound **14d** and **19b**. The inhibition rate of Afatinib and selected compounds **14d** and **19b** against four cancer cell lines increased with elevated concentration. The results indicated that the target compounds inhibited the growth of the four tumor cell lines in a concentration-dependent manner (Fig. 3).

3.4. Morphologic changes of A549 cells under inverted microscopy and fluorescence microscopy

To explain the inhibition of cell growth, the apoptotic experiment by acridine orange (AO) single staining would be carried out to exam the effect of compounds **14d** and **19b** on A549 cell. As shown in Fig. 4, the control group cell (Fig. 4(a)) was stained with acridine orange (AO) and the shape of the cell was full and the edge was clear. But in the other groups (Fig. 4(b and c)) treated with **14d** and **19b**, the shape of which was abnormal with cell shrinkage, chromatin condensation or decomposition into

fragments of varying sizes. This phenomenon indicated that compounds **14d** and **19b** can induce A549 cell apoptosis.

3.5. Cell cycle analysis

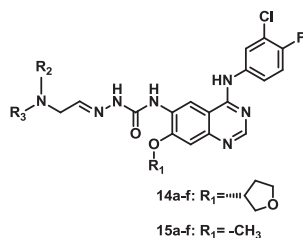
Aiming to better elucidate the relationship between the mechanism of inhibition of proliferation and cell cycle arrest, cells cycle distribution on A549 cells by treating with 4.20 μM **14d** and 5.38 μM **19b** were performed. The data for each phase of the cell cycle was shown in Table 6, on the other hand, area parameter histogram and quantized area parameter histogram were shown in Fig. 5 and Fig. 6, respectively. The region marked with different colors represents % population at different phases of the cell cycle. As can be seen, the percentage of cells in G₂/M phase was increased from 18.21 to 47.45 (Afatinib), 23.62 (**14d**) and 22.31 (**19b**) respectively. And the index of Coefficient of Variation (CV) of G₁ and G₂ were below 7%, indicating that the data was reliable. These results indicated that compounds **14d** and **19b** can inhibit tumor cell proliferation and lead to apoptosis by blocking the cell cycle.

3.6. Molecular docking study

To explore the binding modes of target compounds with the active site of EGFR, molecular docking simulation studies were carried out by using SYBYL6.9.1 (Tripos, St. Louis, USA). Based on the in vitro inhibition results, we selected compound **19b**, the most potent compounds in this study, as ligand example, and the structure of EGFR was selected as the docking model (PDB ID code: 4G5P [22]).

The binding models of compound **19b** with EGFR and the comparison with that of Afatinib are shown in Fig. 7. Two hydrogen bonds were formed with lengths of 1.8 Å (nitrogen of pyrimidine moiety with MET-793 residue) and 2.5 Å (oxygen atom of semicarbazone moiety CYS-797 residue) respectively. In addition, the small molecular amines on the pyrrole extend into the hydrophilic region. As shown in

Table 2
Structures and activity of target compounds **14a–f** and **15a–f**.



Compd.		IC ₅₀ ^a (μM)				LogD _{7.4} ^c
		A549	HepG2	PC-3	MCF-7	
14a		5.62±0.04	3.26±0.01	3.39±0.12	1.08±0.04	2.60
14b		5.38±0.01	3.08±0.08	6.51±0.21	5.72±0.15	2.54
14c		4.32±0.03	2.38±0.03	0.58±0.01	2.34±0.03	2.91
14d		4.20±0.03	0.42±0.01	0.81±0.01	1.53±0.18	3.44
14e		6.48±0.81	2.09±0.02	3.89±0.59	3.12±0.29	2.94
14f		4.34±0.04	3.28±0.02	1.83±0.13	2.04±0.05	2.13
15a		6.69±0.02	4.42±0.64	3.30±0.45	7.43±0.24	2.69
15b		5.52±0.03	2.08±0.02	2.78±0.23	5.38±0.13	2.63
15c		6.19±0.03	2.15±0.02	4.40±0.23	3.28±0.14	3.01
15d		5.63±0.04	2.06±0.02	5.76±0.30	6.42±0.01	3.54
15e		5.67±0.04	2.48±0.01	2.55±0.03	7.53±0.14	3.03
15f		6.60±0.04	2.23±0.08	5.03±0.04	8.76±0.43	2.23
Afatinib^b	-	6.34±0.01	1.16±0.06	1.13±0.05	1.09±0.01	2.34

^a Values are presented as the mean ± SD in two independent experiments.

^bUsed as a positive control.

^cThe result is predicted by <https://chemaxon.com/#/calculation>.

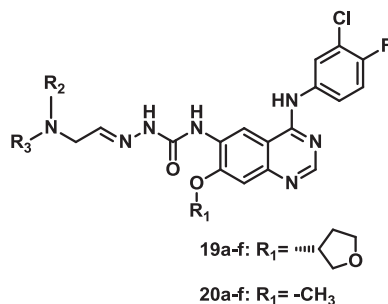
Fig. 7b, compound **19b** and Afatinib nearly overlap in the binding model, it showed that the binding mode of **19b** to EGFR protein is similar to that of Afatinib. Afatinib formed a 2.4 Å hydrogen bond through the interaction of 1-N from quinazoline moiety with residues MET-793 and a covalent bond with Cys797, which is longer than that formed by compound **19b**. Therefore, the hydrogen bond formed by **19b** is stronger than that of Afatinib. The docking study verified that the semicarbazone moiety is in a position that allow it to form a hydrogen bond with Cys797, which may contribute to the potent kinase inhibition activity. Collectively, the SARs analysis and molecular docking study may enlighten rational design of more potent EGFR inhibitors in our later studies.

4. Conclusions

In summary, we designed and synthesized six series (**10a–e**, **11a–e**, **14a–f**, **15a–f**, **19a–l** and **20a–l**) compounds of quinazoline

derivatives containing semicarbazone scaffolds and evaluated the bio-activity. The target compounds (**14a–f**, **15a–f**, **19a–l** and **20a–l**) exhibited excellent cytotoxic activities with the IC₅₀ values reaching nanomolar range against A549, HepG2, MCF-7 and PC-3 cell lines. Further, EGFR^{WT} and EGFR^{L858R/T790M} kinase inhibition assays revealed that the inhibitory activity of two particularly potent compounds (**14d** and **19b**) were equally to or more active than the positive control Afatinib. Moreover, AO staining and cell cycle analysis further evidenced the efficacy of **14d** and **19b** in inducing cell apoptosis and arresting G2/M phase in A549 cell line. In addition, docking studies discovered similar EGFR binding models of **19b** and Afatinib. Altogether, These findings presented herein show the noncovalent inhibitor **14d** and **19b** have the potential to target EGFR mutants. The results also provide more insights for designing new classes of mutant selective EGFR inhibitors. We intend to investigate the PK parameters of some representative compounds in future work to look at logP, solubility, clearance, hERG inhibition [23] and so on.

Table 3
EGFR kinase inhibitory activity of compounds **14a**, **14b**, **14c**, **14d**, **14f** and Afatinib.



Compd.	R ₁		EGFR IC ₅₀ ^a (nM)	
			WT	L858R/T790M
14a			1.5±0.05	14.3±0.3
14b			0.2±0.02	15.4±0.4
14c			0.4±0.04	13.2±0.3
14d			0.1±0.01	8.6±0.12
14f			1.8±0.01	11.6±0.12
Afatinib^b	-	-	4.0±0.18	3.8±0.03

^a Values are presented as the mean ± SD in two independent experiments.

^b Used as a positive control.

5. Experimental

5.1. Chemistry

Unless otherwise mentioned, all the chemicals and materials were purchased from commercially available suppliers and were used directly without the further purifications. All melting points were obtained on a Büchi Melting Point B- 540 apparatus (Büchi Labortechnik, Flawil, Switzerland) and were uncorrected. NMR spectra were performed using Bruker 400 MHz spectrometers (Bruker Bioscience, Billerica, MA, USA) with TMS as an internal standard. Mass spectra (MS) were taken in ESI mode on Agilent 1100 LC-MS (Agilent, Palo Alto, CA, USA). TLC analysis was carried out on silica gel plates GF254 (Qindao Haiyang Chemical, China). Compounds **1-8a**, **8b** were prepared by adapting published procedures [10,20].

5.2. General procedure for the preparation of target compounds **10a-e** and **11a-e**

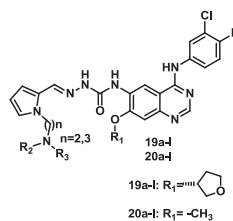
To a solution of **8a-b** (0.46 mmol) in ethanol (6 mL), 1.1 equiv. of aldehydes and acetic acid (1 drop) were added, and the mixture was refluxed for 9–10 h until TLC showed the completion of the

reaction. After cooling to room temperature, the precipitate was filtered and dried in vacuo to obtain the corresponding target compounds **10a-e** and **11a-e** which were purified by washing with isopropanol (3 × 5 mL).

BMC201725-9o: (*S,E*)-*N*-(4-((3-chloro-4-fluorophenyl)amino)-7-((tetrahydrofuran-3-yl)oxy)quinazolin-6-yl)-2-(4-hydroxybenzylidene)hydrazine carboxamide.

5.2.1. (*S,E*)-*N*-(4-((3-chloro-4-fluorophenyl)amino)-7-((tetrahydrofuran-3-yl)oxy)quinazolin-6-yl)-2-(furan-2-ylmethylene)hydrazine carboxamide (**10a**)

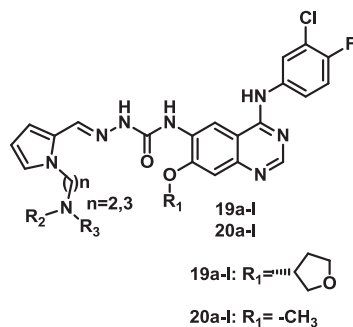
White solid; mp 303.4–304.5 °C; yield: 56.4%; ¹H NMR (400 MHz, DMSO-*d*₆) δ 11.15 (s, 1H), 9.85 (s, 1H), 9.15 (s, 1H), 8.97 (s, 1H), 8.50 (s, 1H), 8.08 (d, *J* = 7.1 Hz, 1H), 7.91 (s, 1H), 7.80 (s, 2H), 7.41 (t, *J* = 9.1 Hz, 1H), 7.30 (s, 1H), 6.90 (s, 1H), 6.65 (s, 1H), 5.42 (s, 1H), 4.01 (t, *J* = 11.3 Hz, 3H), 3.88 (d, *J* = 4.2 Hz, 1H), 2.40 (dd, *J* = 14.1, 6.4 Hz, 1H), 2.23 (s, 1H); ESI-MS *m/z*: [M + H]⁺ 511.1. Analytical HPLC on an Agilent (1260) using C18 analytical column, H₂O/C₂H₃N (0.1%TFA) eluent at 1 mL/min flow, monitored by UV absorption at 254 nm, showed 96.3% purity.

Table 4Structures and activity of target compounds **19a–I** and **20a–I**.

Compd.	n		IC ₅₀ ^a (μM)				LogD _{7.4} ^c
			A549	HepG2	PC-3	MCF-7	
19a	2		1.32±0.03	1.68±0.03	4.27±0.15	2.13±0.12	3.86
19b	2		1.84±0.05	0.04±0.01	3.84±0.38	4.82±0.28	2.59
19c	2		1.59±0.02	0.54±0.01	0.15±0.01	1.28±0.10	2.78
19d	2		3.58±0.04	0.59±0.01	1.57±0.19	2.41±0.18	3.26
19e	2		2.39±0.07	0.64±0.01	1.90±0.28	1.20±0.08	2.69
19f	2		3.02±0.08	0.15±0.01	1.89±0.08	2.42±0.38	3.33
19g	3		5.62±0.01	1.89±0.07	6.32±0.42	5.57±0.51	3.69
19h	3		6.17±0.09	1.37±0.03	3.74±0.13	6.17±0.20	2.05
19i	3		2.36±0.03	0.71±0.01	2.24±0.35	2.49±0.19	2.28
19j	3		2.44±0.08	0.52±0.01	0.15±0.01	1.32±0.02	2.81
19k	3		4.36±0.03	0.67±0.01	1.82±0.26	2.41±0.18	2.25
19l	3		4.06±0.08	0.68±0.01	2.06±0.11	2.12±0.22	3.05
20a	2		0.58±0.02	0.03±0.01	0.82±0.01	1.17±0.07	4.31
20b	2		4.30±0.01	0.11±0.01	1.25±0.09	3.21±0.10	3.05
20c	2		0.43±0.01	1.62±0.01	1.05±0.12	0.57±0.13	3.24
20d	2		2.31±0.08	0.05±0.02	2.24±0.23	2.18±0.27	3.36
20e	2		0.35±0.02	0.16±0.01	1.24±0.11	2.45±0.23	2.79
20f	2		2.34±0.01	0.22±0.03	2.08±0.10	1.85±0.15	3.43
20g	3		1.86±0.02	0.12±0.01	0.05±0.01	1.44±0.10	4.14
20h	3		2.00±0.01	0.05±0.03	0.03±0.01	1.26±0.10	2.51
20i	3		2.38±0.01	0.22±0.01	1.18±0.02	2.43±0.14	2.74
20j	3		3.08±0.04	0.31±0.02	1.06±0.01	2.81±0.04	3.27
20k	3		2.45±0.02	0.06±0.02	1.56±0.02	1.33±0.12	2.71
20l	3		3.23±0.01	0.08±0.01	0.66±0.08	2.43±0.10	3.51
Afatinib ^b	-	-	6.34±0.01	1.16±0.06	1.13±0.05	1.09±0.01	2.34

^a Values are presented as the mean ± SD in two independent experiments.^b Used as a positive control.^c The result is predicted by [https:// chemaxon.com /#/calculation](https://chemaxon.com/#/calculation).

Table 5
EGFR kinase inhibitory activity of compounds **19a**, **19b**, **19i**, **19j**, **20b**, **20h** and Afatinib.



Compd.	n	R ₁		EGFR IC ₅₀ ^a (nM)	
				WT	L858R/T790M
19a	2			0.60±0.04	16.7±0.06
19b	2			0.05±0.01	5.6±0.08
19i	3			0.50±0.04	12.8±0.16
19j	3			0.80±0.04	11.4±0.12
20b	2	-CH ₃		0.10±0.01	21.7±0.18
20h	3	-CH ₃		1.20±0.02	24.3±0.24
Afatinib^b	-	-	-	4.0±0.18	3.8±0.03

^a Values are presented as the mean ± SD in two independent experiments.

^b Used as a positive control.

5.2.2. (*S,E*)-*N*-(4-((3-chloro-4-fluorophenyl)amino)-7-((tetrahydrofuran-3-yl)oxy)quinazolin-6-yl)-2-((5-methylfuran-2-yl)methylene)hydrazine carboxamide (**10b**)

White solid; mp 268.4–269.5 °C; yield: 64.2%; ¹H NMR (400 MHz, DMSO-*d*₆) δ 11.05 (s, 1H), 9.85 (s, 1H), 9.11 (s, 1H), 8.99 (s, 1H), 8.50 (s, 1H), 8.07 (d, *J* = 6.5 Hz, 1H), 7.82 (s, 1H), 7.76 (s, 1H), 7.41 (t, *J* = 9.1 Hz, 1H), 7.30 (s, 1H), 6.77 (d, *J* = 2.6 Hz, 1H), 6.27 (s, 1H), 5.41 (s, 1H), 4.03 (m, 3H), 3.86 (d, *J* = 4.7 Hz, 1H), 2.44 (dd, *J* = 14.5, 6.7 Hz, 1H), 2.36 (s, 3H), 2.20 (d, *J* = 6.4 Hz, 1H); ESI-MS *m/z*: [M + H]⁺ 525.1. Analytical HPLC on an Agilent (1260) using C18 analytical column, H₂O/C₂H₅N (0.1%TFA) eluent at 1 mL/min flow, monitored by UV absorption at 254 nm, showed 95.8% purity.

5.2.3. (*S,E*)-*N*-(4-((3-chloro-4-fluorophenyl)amino)-7-((tetrahydrofuran-3-yl)oxy)quinazolin-6-yl)-2-((5-methylthiophen-2-yl)methylene)hydrazine carboxamide (**10c**)

White solid; mp 286.2–287.5 °C; yield: 60.2%; ¹H NMR (400 MHz, DMSO-*d*₆) δ 11.08 (s, 1H), 9.85 (s, 1H), 9.02 (s, 1H), 8.89 (s, 1H), 8.50 (s, 1H), 8.10 (d, *J* = 7.5 Hz, 1H), 8.09 (s, 1H), 7.76 (s, 1H), 7.41 (t, *J* = 9.3 Hz, 1H), 7.29 (s, 1H), 7.23 (s, 1H), 6.84 (s, 1H), 5.42 (s, 1H),

4.13–4.05 (m, 2H), 4.01 (dd, *J* = 12.3, 8.3 Hz, 1H), 3.87 (d, *J* = 4.9 Hz, 1H), 2.47 (s, 3H), 2.45–2.36 (m, 1H), 2.26 (s, 1H); ESI-MS *m/z*: [M + H]⁺ 542.1.

5.2.4 (*S,E*)-*N*-(4-((3-chloro-4-fluorophenyl)amino)-7-((tetrahydrofuran-3-yl)oxy)quinazolin-6-yl)-2-((5-ethylthiophen-2-yl)methylene)hydrazine carboxamide (**10d**)

White solid; mp 289.4–290.5 °C; yield: 72.2%; ¹H NMR (400 MHz, DMSO-*d*₆) δ 11.10 (s, 1H), 9.85 (s, 1H), 9.03 (s, 1H), 8.91 (s, 1H), 8.50 (s, 1H), 8.13 (s, 1H), 8.08 (d, *J* = 6.2 Hz, 1H), 7.76 (s, 1H), 7.41 (t, *J* = 9.1 Hz, 1H), 7.30 (s, 1H), 7.25 (s, 1H), 6.87 (s, 1H), 5.43 (s, 1H), 4.09 (s, 2H), 3.99 (t, *J* = 7.6 Hz, 1H), 3.87 (d, *J* = 4.7 Hz, 1H), 2.84 (q, *J* = 7.2 Hz, 2H), 2.43 (dd, *J* = 13.6, 6.9 Hz, 1H), 2.26 (s, 1H), 1.28–1.22 (m, 3H); ESI-MS *m/z*: [M + H]⁺ 556.1.

5.2.5 (*S,E*)-2-((1*H*-pyrrol-2-yl)methylene)-*N*-(4-((3-chloro-4-fluorophenyl)amino)-7-((tetrahydrofuran-3-yl)oxy)quinazolin-6-yl)hydrazine carboxamide (**10e**)

Yellow solid; yield: 74.5%; ¹H NMR (400 MHz, DMSO-*d*₆) δ 11.25 (s, 1H), 10.83 (s, 1H), 9.84 (s, 1H), 8.99 (s, 1H), 8.88 (s, 1H), 8.50 (d, *J* = 6.6 Hz, 1H), 8.11 (dd, *J* = 6.8, 2.5 Hz, 1H), 7.87 (s, 1H), 7.82–7.75 (m,

1H), 7.42 (t, $J = 9.1$ Hz, 1H), 7.32 (s, 1H), 6.95 (s, 1H), 6.49 (s, 1H), 6.15 (d, $J = 2.5$ Hz, 1H), 5.41 (s, 1H), 4.02 (dd, $J = 12.3, 7.1$ Hz, 2H), 3.95 (dt, $J = 15.8, 5.9$ Hz, 1H), 3.81 (td, $J = 8.4, 4.7$ Hz, 1H), 3.48–3.39 (m, 1H), 2.36 (td, $J = 14.1, 8.1$ Hz, 1H), 2.19–2.10 (m, 1H); ESI-MS m/z : $[M + H]^+$ 510.1. Analytical HPLC on an Agilent (1260) using C18 analytical column, H_2O/C_2H_5N (0.1%TFA) eluent at 1 mL/min flow, monitored by UV absorption at 254 nm, showed 96.4% purity.

5.2.6 (*E*)-*N*-(4-((3-chloro-4-fluorophenyl)amino)-7-methoxyquinazolin-6-yl)-2-(furan-2-ylmethylene)hydrazine carboxamide (**11a**)

White solid; mp 292.4–293.3 °C; yield: 65.2%; 1H NMR (400 MHz, DMSO- d_6) δ 11.10 (s, 1H), 9.83 (s, 1H), 8.93 (s, 1H), 8.88 (s, 1H), 8.51 (s, 1H), 8.09 (d, $J = 6.6$ Hz, 1H), 7.92 (s, 1H), 7.85 (s, 1H), 7.77 (s, 1H), 7.41 (t, $J = 9.5$ Hz, 1H), 7.32 (s, 1H), 6.91 (s, 1H), 6.65 (s, 1H), 4.09 (s, 3H); ESI-MS m/z : $[M + H]^+$ 455.1.

5.2.7 (*E*)-*N*-(4-((3-chloro-4-fluorophenyl)amino)-7-methoxyquinazolin-6-yl)-2-((5-methylfuran-2-yl)methylene)hydrazine carboxamide (**11b**)

White solid; mp 272.2–273.3 °C; yield: 64.3%; 1H NMR (400 MHz, DMSO- d_6) δ 11.01 (s, 1H), 9.82 (s, 1H), 8.93 (s, 2H), 8.51 (s, 1H), 8.09 (d, $J = 6.5$ Hz, 1H), 7.82 (d, $J = 5.1$ Hz, 1H), 7.77 (s, 1H), 7.41 (t, $J = 9.0$ Hz, 1H), 7.32 (s, 1H), 6.78 (s, 1H), 6.27 (s, 1H), 4.09 (s, 3H), 2.37 (s, 3H); ESI-MS m/z : $[M + H]^+$ 469.1.

5.2.8 (*E*)-*N*-(4-((3-chloro-4-fluorophenyl)amino)-7-methoxyquinazolin-6-yl)-2-((5-methylthiophen-2-yl)methylene)hydrazine carboxamide (**11c**)

White solid; mp 284.2–285.3 °C; yield: 72.5%; 1H NMR (400 MHz, DMSO- d_6) δ 11.06 (s, 1H), 9.84 (s, 1H), 8.95 (d, $J = 8.5$ Hz, 2H), 8.51 (s, 1H), 8.09 (d, $J = 9.4$ Hz, 2H), 7.80 (d, $J = 15.5$ Hz, 1H), 7.41 (t, $J = 9.3$ Hz, 1H), 7.32 (s, 1H), 7.24 (s, 1H), 6.84 (s, 1H), 4.12 (s, 3H), 2.51 (s, 3H); ESI-MS m/z : $[M + H]^+$ 485.1.

5.2.9 (*E*)-*N*-(4-((3-chloro-4-fluorophenyl)amino)-7-methoxyquinazolin-6-yl)-2-((5-ethylthiophen-2-yl)methylene)hydrazine carboxamide (**11d**)

White solid; mp 269.2–270.5 °C; yield: 75.3%; 1H NMR (400 MHz, DMSO- d_6) δ 11.07 (s, 1H), 9.83 (s, 1H), 8.98 (s, 1H), 8.93 (s, 1H), 8.51 (s, 1H), 8.12 (s, 2H), 7.78 (d, $J = 8.5$ Hz, 1H), 7.41 (t, $J = 9.1$ Hz, 1H), 7.32 (s, 1H), 7.25 (d, $J = 3.6$ Hz, 1H), 6.87 (s, 1H), 4.12 (s, 3H), 2.85 (d, $J = 7.4$ Hz, 2H), 1.28 (t, $J = 7.5$ Hz, 3H); ESI-MS m/z : $[M + H]^+$ 499.1.

5.2.10 (*E*)-2-((1*H*-pyrrol-2-yl)methylene)-*n*-(4-((3-chloro-4-fluorophenyl)amino)-7-methoxyquinazolin-6-yl)hydrazine carboxamide (**11e**)

Yellow solid; yield: 78.3%; 1H NMR (400 MHz, DMSO- d_6) δ 11.44 (s, 1H), 10.74 (s, 1H), 9.81 (s, 1H), 8.80 (s, 1H), 8.53 (s, 1H), 8.13 (dd, $J = 6.9, 2.6$ Hz, 1H), 7.83 (d, $J = 11.9$ Hz, 2H), 7.82–7.76 (m, 1H), 7.42 (t, $J = 9.1$ Hz, 1H), 7.31 (s, 1H), 6.97 (s, 1H), 6.43 (s, 1H), 6.14 (dd, $J = 5.6, 2.5$ Hz, 1H), 4.05 (s, 3H); ESI-MS m/z : $[M + H]^+$ 454.1. Analytical HPLC on an Agilent (1260) using C18 analytical column, H_2O/C_2H_5N (0.1%TFA) eluent at 1 mL/min flow, monitored by UV absorption at 254 nm, showed 97.5% purity.

5.3. General procedure for the preparation of compounds **12a-f**

To a solution of 2-bromo-1,1-diethoxyethane (1.0 mmol) in DMF (3.0 mL), 2.0 equiv. of amines was added, and the mixture was heated to 100 °C for 2 h, respectively. After the reaction completed, the mixture was poured into water and extracted with ethyl acetate, washed with brine and dried with anhydrous Na_2SO_4 and concentrated under reduce pressure to obtained corresponding compounds **12a-f**.

5.4. General procedure for the preparation of compounds **13a-f**

The mixture of **12a-f** (0.56 mmol), concentrated hydrochloric acid (1.5 mL) and water (1.5 mL) was heated to 50 °C for 2 h under nitrogen,

respectively. The solution was used for the next step without further purification.

5.5. General procedure for the preparation of target compounds **14a-f** and **15a-f**

To a solution of **13a-f** (0.56 mmol) in concentrated hydrochloric acid (1.5 mL) and water (1.5 mL), 0.5 equiv. of **8a** or **8b** and ethanol (3.0 mL) were added, and the mixture was heated to 80 °C for 2 h. After confirming the completion of the reaction by thin layer chromatography, The reaction mixture was cooled to room temperature and the solution was alkalinized to pH = 8 to yielding a precipitate. The mixture was filtered and washed with water and the filtrate was concentrated under reduced pressure. The resulting residue was purified via flash column chromatography with dichloromethane / methanol (30:1) to furnish the target compounds **14a-f** and **15a-f**.

5.5.1. (*S,E*)-*N*-(4-((3-chloro-4-fluorophenyl)amino)-7-((tetrahydrofuran-3-yl)oxy)quinazolin-6-yl)-2-(2-morpholinoethylidene)hydrazine carboxamide (**14a**)

Yellow solid; mp 202.4–203.9 °C; yield: 65.2%; 1H NMR (400 MHz, DMSO- d_6) δ 10.92 (s, 1H), 9.86 (d, $J = 12.0$ Hz, 1H), 8.95 (d, $J = 15.3$ Hz, 2H), 8.48 (d, $J = 12.4$ Hz, 1H), 8.08 (s, 1H), 7.75 (d, $J = 15.0$ Hz, 1H), 7.41 (t, $J = 8.9$ Hz, 1H), 7.30 (d, $J = 6.4$ Hz, 2H), 5.41 (s, 1H), 4.04–3.87 (m, 4H), 3.53 (m, 4H), 3.10 (d, $J = 5.0$ Hz, 2H), 2.40 (s, 5H), 2.12 (s, 1H); ESI-MS m/z : $[M + H]^+$ 544.1. Analytical HPLC on an Agilent (1260) using C18 analytical column, H_2O/C_2H_5N (0.1%TFA) eluent at 1 mL/min flow, monitored by UV absorption at 254 nm, showed 94.8% purity.

5.5.2. (*S,E*)-*N*-(4-((3-chloro-4-fluorophenyl)amino)-7-((tetrahydrofuran-3-yl)oxy)quinazolin-6-yl)-2-(2-(dimethylamino)ethylidene)hydrazine carboxamide (**14b**)

Yellow solid; mp 227.8–228.9 °C; yield: 68.3%; 1H NMR (400 MHz, DMSO- d_6) δ 10.86 (s, 1H), 9.84 (s, 1H), 8.95 (d, $J = 14.7$ Hz, 2H), 8.49 (s, 1H), 8.08 (d, $J = 6.6$ Hz, 1H), 7.76 (s, 1H), 7.41 (t, $J = 9.0$ Hz, 1H), 7.36–7.25 (m, 2H), 5.40 (s, 1H), 4.05–3.98 (m, 1H), 3.91 (d, $J = 10.3$ Hz, 2H), 3.86 (d, $J = 4.4$ Hz, 1H), 3.04 (d, $J = 5.3$ Hz, 2H), 2.37 (dd, $J = 13.7, 6.1$ Hz, 1H), 2.19 (s, 6H), 2.12 (s, 1H); ESI-MS m/z : $[M + H]^+$ 502.1. ^{13}C NMR (101 MHz, DMSO- d_6) δ 157.18, 153.48, 152.68, 152.34, 151.21, 147.79, 143.68, 137.41, 128.97, 128.63, 124.02, 122.97, 119.17, 116.89, 109.85, 108.41, 79.32, 72.61, 66.92, 60.80, 45.61(2C), 33.03. Analytical HPLC on an Agilent (1260) using C18 analytical column, H_2O/C_2H_5N (0.1%TFA) eluent at 1 mL/min flow, monitored by UV absorption at 254 nm, showed 97.3% purity.

5.5.3. (*S,E*)-*N*-(4-((3-chloro-4-fluorophenyl)amino)-7-((tetrahydrofuran-3-yl)oxy)quinazolin-6-yl)-2-(2-(diethylamino)ethylidene)hydrazine carboxamide (**14c**)

Yellow solid; mp 197.5–198.6 °C; yield: 71.2%; 1H NMR (400 MHz, DMSO- d_6) δ 10.86 (s, 1H), 9.87 (d, $J = 11.3$ Hz, 1H), 8.95 (d, $J = 10.0$ Hz, 2H), 8.49 (s, 1H), 8.08 (d, $J = 4.7$ Hz, 1H), 7.77 (s, 1H), 7.41 (t, $J = 9.1$ Hz, 1H), 7.37–7.26 (m, 2H), 5.40 (s, 1H), 3.88 (dd, $J = 13.4, 5.3$ Hz, 4H), 3.18 (dd, $J = 10.6, 4.9$ Hz, 6H), 2.36 (dd, $J = 14.0, 6.5$ Hz, 1H), 2.09 (d, $J = 12.5$ Hz, 1H), 0.99 (t, $J = 7.0$ Hz, 6H); ESI-MS m/z : $[M + H]^+$ 530.2. ^{13}C NMR (101 MHz, DMSO- d_6) δ 157.18, 153.48, 152.67, 151.20, 147.79, 144.40, 137.44, 128.97, 124.03, 122.98, 118.98, 116.90, 116.68, 110.04, 109.85, 108.40, 79.29, 72.62, 66.91, 54.64, 47.12(2C), 33.04, 12.11(2C). Analytical HPLC on an Agilent (1260) using C18 analytical column, H_2O/C_2H_5N (0.1%TFA) eluent at 1 mL/min flow, monitored by UV absorption at 254 nm, showed 96.7% purity.

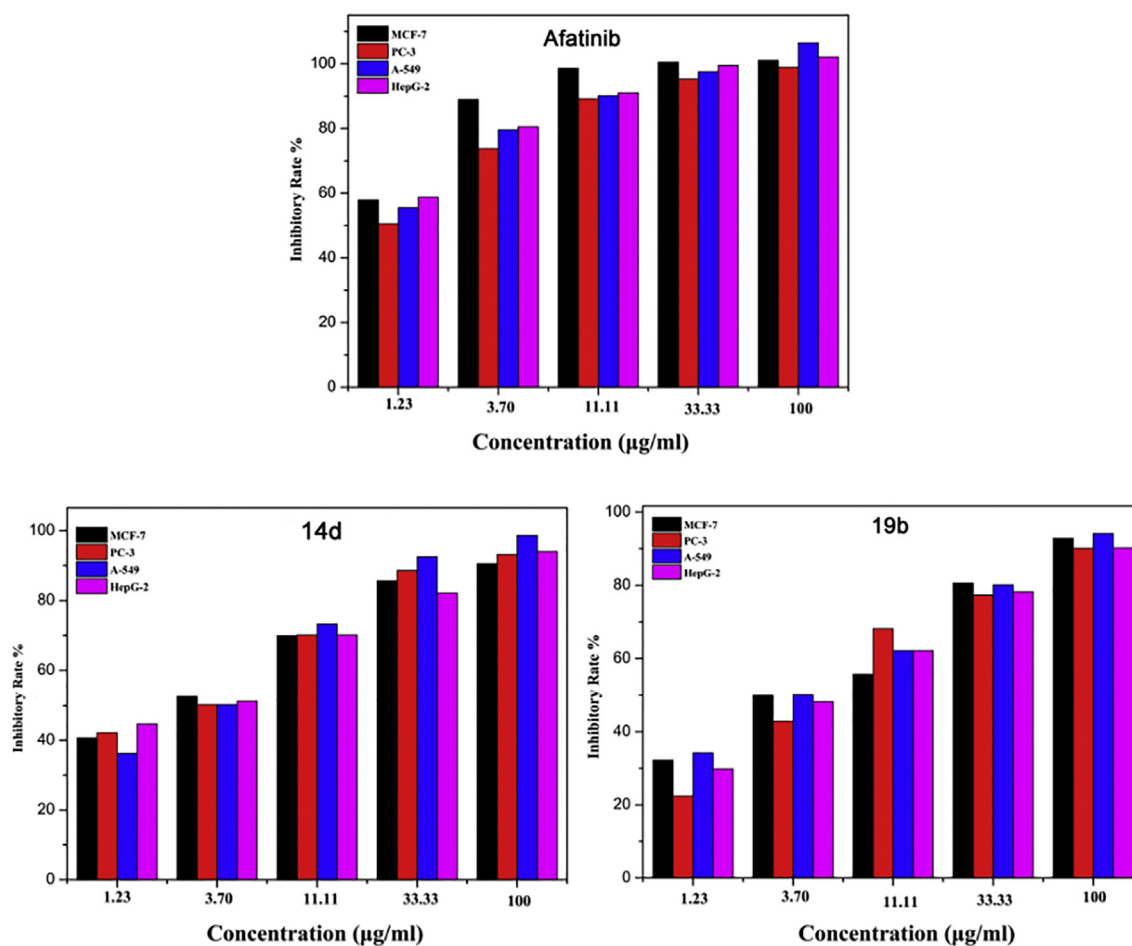


Fig. 3. Relationship between activity and concentration of Afatinib and selected compound **14d** and **19b** against four cancer cell lines.

5.5.4. *(S,E)-N-(4-((3-chloro-4-fluorophenyl)amino)-7-((tetrahydrofuran-3-yl)oxy)quinazolin-6-yl)-2-(2-(piperidin-1-yl)ethylidene)hydrazine carboxamide (14d)*

Yellow solid; mp 211.9–212.8 °C; yield: 68.3%; ¹H NMR (400 MHz, DMSO-*d*₆) δ 10.88 (s, 1H), 9.85 (s, 1H), 8.95 (d, *J* = 18.5 Hz, 2H), 8.49 (s, 1H), 8.08 (s, 1H), 7.77 (s, 1H), 7.46–7.39 (m, 1H), 7.29 (s, 2H), 5.40 (s, 1H), 3.90 (d, *J* = 9.1 Hz, 4H), 3.05 (d, *J* = 5.1 Hz, 2H), 2.36 (s, 5H), 2.12 (s, 1H), 1.51 (s, 4H), 1.39 (s, 2H); ESI-MS *m/z*: [M + H]⁺ 542.2. Analytical HPLC on an Agilent (1260) using C18 analytical column, H₂O/

C₂H₃N (0.1%TFA) eluent at 1 mL/min flow, monitored by UV absorption at 254 nm, showed 97.4% purity.

5.5.5. *(S,E)-N-(4-((3-chloro-4-fluorophenyl)amino)-7-((tetrahydrofuran-3-yl)oxy)quinazolin-6-yl)-2-(2-(pyrrolidin-1-yl)ethylidene)hydrazine carboxamide (14e)*

Yellow solid; mp 203.4–204.7 °C; yield: 65.2%; ¹H NMR (400 MHz, DMSO-*d*₆) δ 10.86 (s, 1H), 9.85 (s, 1H), 8.95 (d, *J* = 11.1 Hz, 2H), 8.50 (d, *J* = 6.8 Hz, 1H), 8.08 (dd, *J* = 6.8, 2.4 Hz, 1H), 7.83–7.74 (m, 1H),

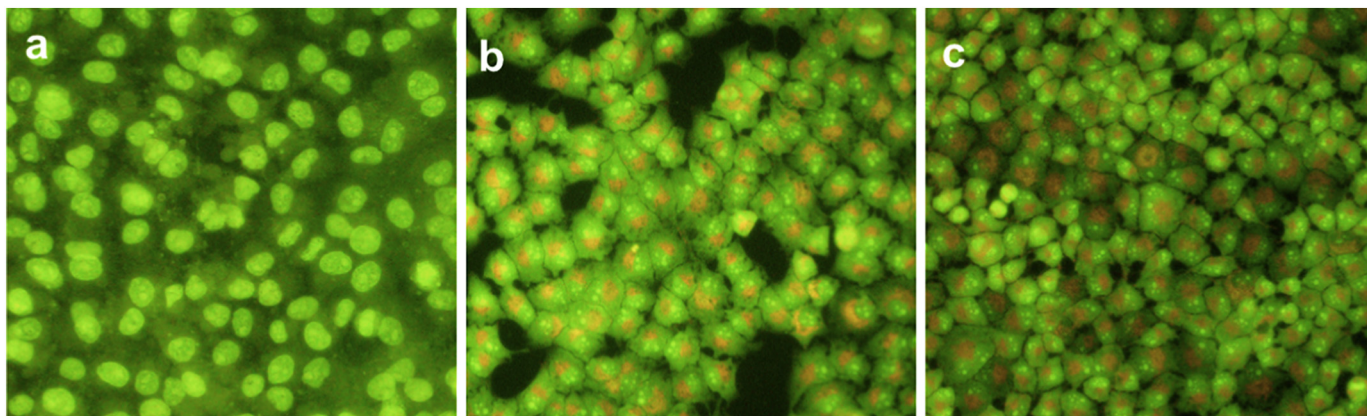


Fig. 4. Morphologic changes of A549 cells observed under inverted microscopy and fluorescence microscopy. (4a): The control group cell treated with nothing; (4b): Experimental group treated with 4.20 µM **14d** for 12 h. (4c): Experimental group treated with 5.38 µM **19b** for 12 h.

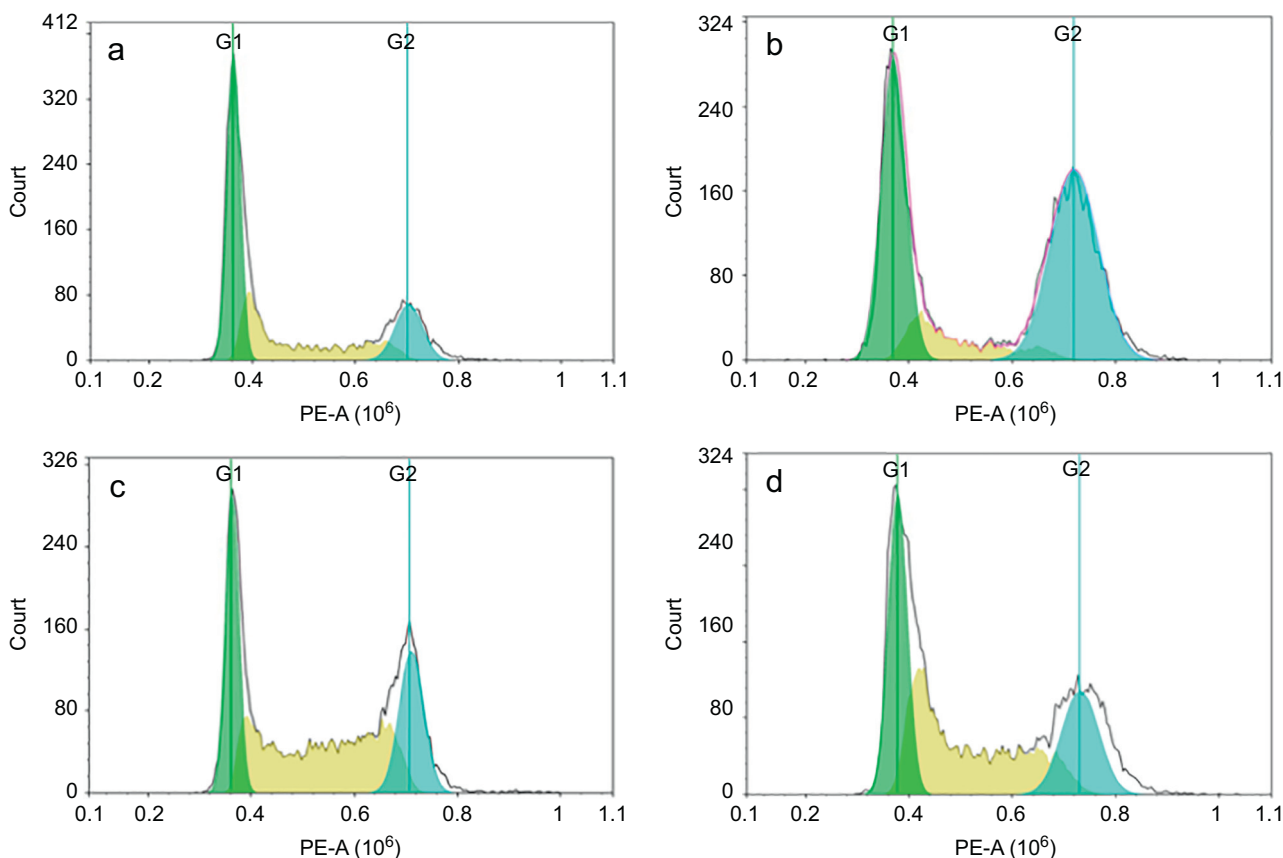


Fig. 5. Cell cycle analysis in A549 cells. (Fig. 5a: control; Fig. 5b: Afatinib treated with A549 cells; 5c: **14d** treated with A549 cells; 5d: **19b** treated with A549 cells.)

7.41 (t, $J = 9.1$ Hz, 1H), 7.37–7.24 (m, 2H), 5.40 (s, 1H), 4.12 (d, $J = 4.7$ Hz, 1H), 4.01 (dd, $J = 10.4, 4.1$ Hz, 1H), 3.89 (dd, $J = 13.3, 6.8$ Hz, 2H), 3.20 (d, $J = 5.5$ Hz, 2H), 3.16 (d, $J = 4.1$ Hz, 4H), 2.36 (dd, $J = 14.0, 5.9$ Hz, 1H), 2.15–2.04 (m, 1H), 1.71 (s, 4H); ESI-MS m/z : $[M + H]^+$ 528.1.

5.5.6. (*S,E*)-*N*-4-((3-chloro-4-fluorophenyl)amino)-7-((tetrahydrofuran-3-yl)oxy)quinazolin-6-yl)-2-(2-(4-methylpiperazin-1-yl)ethylidene)hydrazine carboxamide (**14f**)

Yellow solid; mp 190.5–191.7 °C; yield: 70.2%; ^1H NMR (400 MHz, DMSO- d_6) δ 10.89 (s, 1H), 9.87 (d, $J = 12.2$ Hz, 1H), 8.94 (d, $J = 13.6$ Hz, 2H), 8.50 (d, $J = 6.6$ Hz, 1H), 8.08 (d, $J = 2.5$ Hz, 1H), 7.81–7.73 (m, 1H), 7.42 (dd, $J = 11.1, 7.0$ Hz, 1H), 7.31 (d, $J = 10.6$ Hz, 2H), 5.40 (s, 1H), 4.11 (d, $J = 5.2$ Hz, 1H), 4.02 (dd, $J = 10.3, 4.1$ Hz, 1H), 3.91 (d, $J = 9.5$ Hz, 2H), 3.17 (s, 3H), 3.16 (s, 2H), 2.49–2.23 (m, 6H), 2.19 (s, 1H), 2.15 (s, 3H); ESI-MS m/z : $[M + H]^+$ 557.2.

5.5.7. (*E*)-*N*-4-((3-chloro-4-fluorophenyl)amino)-7-methoxyquinazolin-6-yl)-2-(2-morpholinoethylidene)hydrazine carboxamide (**15a**)

Yellow solid; mp 207.8–208.9 °C; yield: 64.3%; ^1H NMR (400 MHz, DMSO- d_6) δ 10.84 (s, 1H), 9.82 (s, 1H), 8.97–8.76 (m, 2H), 8.49 (d, $J = 12.9$ Hz, 1H), 8.08 (d, $J = 6.0$ Hz, 1H), 7.78 (s, 1H), 7.41 (dd, $J = 11.0,$

6.6 Hz, 1H), 7.35–7.25 (m, 2H), 4.05 (s, 3H), 3.54 (d, $J = 14.2$ Hz, 4H), 3.15 (d, $J = 4.8$ Hz, 2H), 2.44 (s, 4H); ESI-MS m/z : $[M + H]^+$ 488.1.

5.5.8. (*E*)-*N*-4-((3-chloro-4-fluorophenyl)amino)-7-methoxyquinazolin-6-yl)-2-(2-(dimethylamino)ethylidene)hydrazine carboxamide (**15b**)

Yellow solid; mp 226.4–227.9 °C; yield: 68.3%; ^1H NMR (400 MHz, DMSO- d_6) δ 10.71 (s, 1H), 9.71 (s, 1H), 8.80 (s, 1H), 8.66 (s, 1H), 8.38 (s, 1H), 7.96 (d, $J = 6.1$ Hz, 1H), 7.65 (s, 1H), 7.29 (t, $J = 9.0$ Hz, 1H), 7.21 (t, $J = 5.3$ Hz, 1H), 7.17 (s, 1H), 3.93 (s, 3H), 2.96 (d, $J = 5.1$ Hz, 2H), 2.10 (s, 6H); ESI-MS m/z : $[M + H]^+$ 446.1. ^{13}C NMR (101 MHz, DMSO- d_6) δ 157.17, 153.85, 153.55, 152.77, 152.34, 148.13, 144.16, 137.48, 128.43, 124.01, 122.96, 119.17, 116.93, 110.64, 109.85, 106.83, 60.49, 57.06, 45.56(2C). Analytical HPLC on an Agilent (1260) using C18 analytical column, $\text{H}_2\text{O}/\text{C}_2\text{H}_5\text{N}$ (0.1%TFA) eluent at 1 mL/min flow, monitored by UV absorption at 254 nm, showed 94.6% purity.

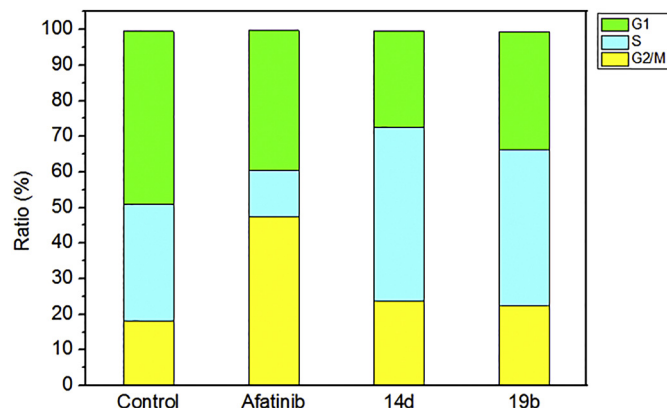


Fig. 6. Cell cycle analysis in A549 cells for Afatinib, compounds **14d** and **19b**.

Table 6
Effects of Afatinib and compounds **14d** and **19b** on the cell cycle against A549 cell lines.

Compounds	RMS	Freq G1	Freq S	Freq G2	CV G1	CV G2	Freq Sub-G1
Control	9.63	48.59	32.62	18.21	3.57%	3.76%	0.07
Afatinib	12.40	39.41	12.92	47.45	6.57%	6.45%	0.03
14d	4.73	27.08	48.44	23.62	3.61%	3.36%	0.06
19b	16.33	33.23	43.84	22.31	4.86%	4.87%	0.05

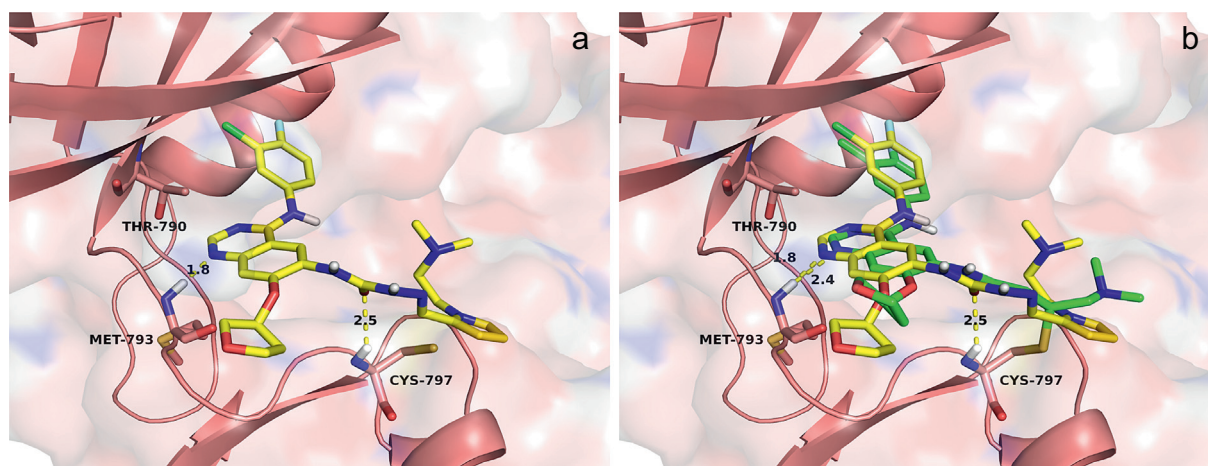


Fig. 7. a: Binding model of compound **19b** with EGFR. b: binding model of compound **19b** and Afatinib with EGFR, respectively. The proteins were displayed by colors ribbon. H-bonding interactions were indicated with dashed lines in yellow.

5.5.9. (*E*)-*N*-(4-((3-chloro-4-fluorophenyl)amino)-7-methoxyquinazolin-6-yl)-2-(2-(diethylamino)ethylidene)hydrazine carboxamide (**15c**)

Yellow solid; mp 196.3–197.8 °C; yield: 70.5%; $^1\text{H NMR}$ (400 MHz, DMSO- d_6) δ 10.81 (s, 1H), 9.83 (s, 1H), 8.91 (s, 1H), 8.82 (d, $J = 19.2$ Hz, 1H), 8.50 (s, 1H), 8.08 (d, $J = 5.2$ Hz, 1H), 7.78 (s, 1H), 7.41 (t, $J = 9.0$ Hz, 1H), 7.30 (d, $J = 5.6$ Hz, 2H), 4.04 (s, 3H), 3.23 (d, $J = 5.1$ Hz, 2H), 2.53 (dd, $J = 11.8, 4.3$ Hz, 4H), 1.00 (t, $J = 7.0$ Hz, 6H); ESI-MS m/z : $[\text{M} + \text{H}]^+$ 474.1. $^{13}\text{C NMR}$ (101 MHz, DMSO- d_6) δ 157.17, 153.75, 153.54, 152.76, 148.14, 144.57, 137.45, 128.43, 124.00, 122.94, 119.17, 116.90, 116.69, 110.47, 109.85, 106.86, 57.04, 54.15, 47.11 (2C), 12.21 (2C). Analytical HPLC on an Agilent (1260) using C18 analytical column, $\text{H}_2\text{O}/\text{C}_2\text{H}_5\text{N}$ (0.1%TFA) eluent at 1 mL/min flow, monitored by UV absorption at 254 nm, showed 95.8% purity.

5.5.10. (*E*)-*N*-(4-((3-chloro-4-fluorophenyl)amino)-7-methoxyquinazolin-6-yl)-2-(2-(piperidin-1-yl)ethylidene)hydrazine carboxamide (**15d**)

Yellow solid; mp 189.3–191.6 °C; yield: 65.5%; $^1\text{H NMR}$ (400 MHz, DMSO- d_6) δ 10.54 (dd, $J = 14.1, 13.2$ Hz, 1H), 9.85 (s, 1H), 8.90 (s, 1H), 8.77 (s, 1H), 8.48 (s, 1H), 8.07 (d, $J = 5.1$ Hz, 1H), 7.82–7.69 (m, 1H), 7.40 (t, $J = 9.1$ Hz, 1H), 7.31 (t, $J = 5.2$ Hz, 1H), 7.28 (s, 1H), 4.04 (s, 3H), 3.08 (d, $J = 5.2$ Hz, 2H), 2.38 (s, 4H), 1.51 (s, 4H), 1.39 (s, 2H); ESI-MS m/z : $[\text{M} + \text{H}]^+$ 486.1.

5.5.11. (*E*)-*N*-(4-((3-chloro-4-fluorophenyl)amino)-7-methoxyquinazolin-6-yl)-2-(2-(pyrrolidin-1-yl)ethylidene)hydrazine carboxamide (**15e**)

Yellow solid; mp 198.1–199.7 °C; yield: 63.2%; $^1\text{H NMR}$ (400 MHz, DMSO- d_6) δ 10.80 (s, 1H), 9.82 (s, 1H), 8.91 (s, 1H), 8.77 (s, 1H), 8.51 (d, $J = 9.1$ Hz, 1H), 8.08 (dd, $J = 6.8, 2.4$ Hz, 1H), 7.82–7.72 (m, 1H), 7.41 (t, $J = 9.1$ Hz, 1H), 7.35 (t, $J = 5.2$ Hz, 1H), 7.29 (s, 1H), 4.04 (s, 3H), 3.24 (d, $J = 5.2$ Hz, 2H), 2.50 (s, 4H), 1.71 (s, 4H); ESI-MS m/z : $[\text{M} + \text{H}]^+$ 472.1. Analytical HPLC on an Agilent (1260) using C18 analytical column, $\text{H}_2\text{O}/\text{C}_2\text{H}_5\text{N}$ (0.1%TFA) eluent at 1 mL/min flow, monitored by UV absorption at 254 nm, showed 94.8% purity.

5.5.12. (*E*)-*N*-(4-((3-chloro-4-fluorophenyl)amino)-7-methoxyquinazolin-6-yl)-2-(2-(4-methylpiperazin-1-yl)ethylidene)hydrazine carboxamide (**15f**)

Yellow solid; mp 189.3–190.6 °C; yield: 68.7%; $^1\text{H NMR}$ (400 MHz, DMSO- d_6) δ 10.83 (s, 1H), 9.83 (s, 1H), 8.91 (s, 1H), 8.77 (s, 1H), 8.51 (d, $J = 9.1$ Hz, 1H), 8.08 (d, $J = 6.3$ Hz, 1H), 7.78 (s, 1H), 7.42 (dd, $J = 11.5, 6.7$ Hz, 1H), 7.32 (d, $J = 14.5$ Hz, 2H), 4.05 (s, 3H), 3.16 (d, $J = 5.0$ Hz, 4H), 3.13 (d, $J = 5.2$ Hz, 2H), 2.45–2.27 (m, 4H), 2.17 (s, 3H); ESI-MS m/z : $[\text{M} + \text{H}]^+$ 501.1.

5.6. Preparation of 1*H*-pyrrole-2-carbaldehyde (**16**)

DMF (55.0 mmol) was slowly treated with POCl_3 (55.0 mmol) in an ice bath. After completed, the mixture was stirred for 15 min and the ice bath was replaced, and anhydrous 1,2-dichloroethane (13.0 mL) was added, followed by a solution of pyrrole (50.0 mmol) in 1,2-dichloroethane (13.0 mL) over 60 min. The mixture was refluxed for 15 min and then cooled to room temperature. A saturated aqueous NaOAc solution (27.5 mmol NaOAc in 55.0 mL water) was added, and the mixture was refluxed for 20 min. The mixture was cooled to room temperature and then was diluted with ethyl acetate. The mixture was washed with saturated aqueous NaHCO_3 solution. The organic layer was dried with anhydrous Na_2SO_4 and concentrated to yield a brown solid [15] (40.0 mmol, 80%). The solid was used directly without the further purifications. $^1\text{H NMR}$ (400 MHz, DMSO- d_6) δ 6.28–6.38 (m, 1H), 7.03–7.06 (m, 1H), 7.16–7.22 (m, 1H), 9.53 (d, $J = 2.6$ Hz, 1H), 10.62 (m, 1H).

5.7. General procedure for the preparation of compounds **17a–b**

To the mixture of compound **16** (18.5 mmol) in anhydrous DMSO (15.0 mL), 60% NaH (20.5 mmol) was slowly added to the solution at room temperature. The mixture was stirred at room temperature for 1 h. 1-Bromo-2-chloroethane (18.5 mmol) or 1-Bromo-3-chloropropane (18.5 mmol) was added at room temperature and stirred for 1.5 h. After the reaction completed, the reaction mixture was slowly poured into water and extracted with ethyl acetate. The organic layer was dried with anhydrous Na_2SO_4 and concentrated under reduce pressure to obtained a yellow oil liquid, respectively. The oil liquid was purified via column chromatography with petroleum ether/ethyl acetate (3:1), respectively. **17a**: $^1\text{H NMR}$ (400 MHz, DMSO- d_6) $\delta = 9.51$ (s, 1H), 7.05–6.01 (m, 2H), 6.25 (t, $J = 2.6$ Hz, 1H), 4.67 (t, $J = 5.8$ Hz, $J = 5.4$ Hz, 2H), 3.81 (t, $J = 5.4$ Hz, 2H).

5.8. General procedure for the preparation of compounds **18a–L**

Compounds **17a–b** (1.3 mmol) and amines (2.6 mmol) in DMSO (4.0 mL) was heated to 100 °C for 5 h, respectively. After the reaction completed, the mixture was poured into water and extracted with ethyl acetate, washed with brine and was concentrated under reduced pressure, respectively. The resulting residue was purified via column chromatography with dichloromethane / methanol (30:1) dried to obtain the corresponding compounds **18a–l**.

5.9. General procedure for the preparation of target compounds **19a-I** and **20a-I**

To a solution of **18a-I** (0.46 mmol) in DMSO (6.0 mL), 1.1 equiv. of aldehydes and concentrated sulfuric acid (1 drop) were added, and the mixture was heated to 70 °C for 5 h. After the reaction completed, the reaction mixture was cooled to room temperature and the solution was alkalinized to pH = 8 to yielding a precipitate. The mixture was filtered and washed with water and the filtrate was concentrated under reduced pressure. The resulting residue was purified via flash column chromatography with dichloromethane / methanol (30:1) to furnish the target compounds **19a-I** and **20a-I**.

5.9.1. (S,E)-N-(4-((3-chloro-4-fluorophenyl)amino)-7-((tetrahydrofuran-3-yl)oxy)quinazolin-6-yl)-2-((1-(2-morpholinoethyl)-1H-pyrrol-2-yl)methylene)hydrazine carboxamide (**19a**)

Yellow solid; mp 160.2–161.3 °C; yield: 53.4%; ¹H NMR (400 MHz, DMSO-*d*₆) δ 10.77 (d, *J* = 17.3 Hz, 1H), 9.84 (s, 1H), 8.96 (d, *J* = 15.7 Hz, 1H), 8.68 (s, 1H), 8.51 (s, 1H), 8.11 (d, *J* = 6.5 Hz, 1H), 7.99 (t, *J* = 15.1 Hz, 1H), 7.78 (s, 1H), 7.42 (t, *J* = 9.2 Hz, 1H), 7.31 (s, 1H), 7.01 (d, *J* = 19.0 Hz, 1H), 6.53 (s, 1H), 6.11 (s, 1H), 5.40 (s, 1H), 4.31 (s, 2H), 3.92 (m, 4H), 3.40 (m, 4H), 2.56 (s, 2H), 2.45 (s, 1H), 2.35 (s, 4H), 2.09 (s, 1H); ESI-MS *m/z*: [M + H]⁺ 624.2. Analytical HPLC on an Agilent (1260) using C18 analytical column, H₂O/C₂H₅N (0.1%TFA) eluent at 1 mL/min flow, monitored by UV absorption at 254 nm, showed 97.4% purity.

5.9.2. (S,E)-N-(4-((3-chloro-4-fluorophenyl)amino)-7-((tetrahydrofuran-3-yl)oxy)quinazolin-6-yl)-2-((1-(2-(dimethylamino)ethyl)-1H-pyrrol-2-yl)methylene)hydrazine carboxamide (**19b**)

Yellow solid; mp 176.4–177.3 °C; yield: 50.3%; ¹H NMR (400 MHz, DMSO-*d*₆) δ 10.77 (s, 1H), 9.83 (s, 1H), 8.93 (s, 1H), 8.77 (s, 1H), 8.50 (s, 1H), 8.10 (d, *J* = 6.5 Hz, 1H), 7.99 (s, 1H), 7.79 (s, 1H), 7.41 (t, *J* = 9.0 Hz, 1H), 7.29 (s, 1H), 7.00 (d, *J* = 13.0 Hz, 1H), 6.54 (s, 1H), 6.10 (d, *J* = 2.4 Hz, 1H), 5.38 (s, 1H), 4.27 (s, 2H), 3.98 (t, *J* = 6.2 Hz, 2H), 3.97–3.87 (m, 1H), 3.79 (d, *J* = 4.7 Hz, 1H), 2.48 (s, 2H), 2.47–2.16 (m, 2H), 2.11 (s, 6H); ESI-MS *m/z*: [M + H]⁺ 582.2. ¹³C NMR (101 MHz, DMSO-*d*₆) δ 157.16, 153.64, 152.91, 152.35, 152.02, 148.04, 137.41, 135.31, 128.86, 127.41, 126.85, 123.98, 122.91, 119.01, 116.93, 116.72, 111.79, 109.89, 108.86, 108.41, 79.38, 72.75, 67.01, 60.25, 46.46, 45.77 (2C), 32.93. Analytical HPLC on an Agilent (1260) using C18 analytical column, H₂O/C₂H₅N (0.1%TFA) eluent at 1 mL/min flow, monitored by UV absorption at 254 nm, showed 96.8% purity.

5.9.3. (S,E)-N-(4-((3-chloro-4-fluorophenyl)amino)-7-((tetrahydrofuran-3-yl)oxy)quinazolin-6-yl)-2-((1-(2-(diethylamino)ethyl)-1H-pyrrol-2-yl)methylene)hydrazine carboxamide (**19c**)

Yellow solid; mp 131.4–132.3 °C; yield: 52.1%; ¹H NMR (400 MHz, DMSO-*d*₆) δ 10.79 (d, *J* = 14.1 Hz, 1H), 9.85 (s, 1H), 8.98 (s, 1H), 8.71 (s, 1H), 8.50 (s, 1H), 8.10 (d, *J* = 4.4 Hz, 1H), 8.01 (d, *J* = 14.0 Hz, 1H), 7.82–7.73 (m, 1H), 7.42 (t, *J* = 9.0 Hz, 1H), 7.30 (s, 1H), 7.00 (d, *J* = 12.5 Hz, 1H), 6.55 (d, *J* = 15.0 Hz, 1H), 6.11 (d, *J* = 2.8 Hz, 1H), 5.40 (s, 1H), 4.24 (d, *J* = 6.1 Hz, 2H), 4.00 (s, 2H), 3.97–3.85 (m, 1H), 3.80 (d, *J* = 4.8 Hz, 1H), 2.61 (t, *J* = 6.6 Hz, 2H), 2.41 (dd, *J* = 14.1, 7.0 Hz, 5H), 2.15–2.05 (m, 1H), 0.82 (t, *J* = 7.0 Hz, 6H); ESI-MS *m/z*: [M + H]⁺ 609.2. Analytical HPLC on an Agilent (1260) using C18 analytical column, H₂O/C₂H₅N (0.1%TFA) eluent at 1 mL/min flow, monitored by UV absorption at 254 nm, showed 95.1% purity.

5.9.4. (S,E)-N-(4-((3-chloro-4-fluorophenyl)amino)-7-((tetrahydrofuran-3-yl)oxy)quinazolin-6-yl)-2-((1-(2-(piperidin-1-yl)ethyl)-1H-pyrrol-2-yl)methylene)hydrazine carboxamide (**19d**)

Yellow solid; mp 141.2–142.6 °C; yield: 48.4%; ¹H NMR (400 MHz, DMSO-*d*₆) δ 10.79 (s, 1H), 9.85 (s, 1H), 8.96 (d, *J* = 13.1 Hz, 1H), 8.69 (s, 1H), 8.51 (s, 1H), 8.10 (d, *J* = 5.1 Hz, 1H), 7.98 (s, 1H), 7.78 (s, 1H), 7.42 (t, *J* = 8.9 Hz, 1H), 7.30 (s, 1H), 7.00 (d, *J* = 14.7 Hz, 1H), 6.52 (s,

1H), 6.11 (s, 1H), 5.39 (s, 1H), 4.31 (s, 2H), 3.99 (s, 2H), 3.93 (d, *J* = 8.1 Hz, 1H), 3.80 (d, *J* = 5.4 Hz, 1H), 2.54 (s, 2H), 2.46–2.37 (m, 1H), 2.32 (s, 4H), 2.11 (d, *J* = 6.7 Hz, 1H), 1.32 (s, 4H), 1.25 (s, 2H); ESI-MS *m/z*: [M + H]⁺ 622.2.

5.9.5. (S,E)-N-(4-((3-chloro-4-fluorophenyl)amino)-7-((tetrahydrofuran-3-yl)oxy)quinazolin-6-yl)-2-((1-(2-(pyrrolidin-1-yl)ethyl)-1H-pyrrol-2-yl)methylene)hydrazinecarboxamide (**19e**)

Yellow solid; mp 135.1–136.6 °C; yield: 46.2%; ¹H NMR (400 MHz, DMSO-*d*₆) δ 10.79 (s, 1H), 9.84 (s, 1H), 8.91 (s, 1H), 8.75 (s, 1H), 8.51 (s, 1H), 8.12 (d, *J* = 6.8 Hz, 1H), 7.98 (s, 1H), 7.78 (s, 1H), 7.42 (t, *J* = 9.2 Hz, 1H), 7.29 (s, 1H), 7.03 (s, 1H), 6.53 (s, 1H), 6.10 (s, 1H), 5.38 (s, 1H), 4.31 (s, 2H), 4.01–3.95 (m, 2H), 3.92 (s, 1H), 3.80 (d, *J* = 5.0 Hz, 1H), 2.68 (s, 2H), 2.40 (s, 4H), 2.36–2.30 (m, 1H), 2.11 (s, 1H), 1.48 (s, 4H); ESI-MS *m/z*: [M + H]⁺ 608.2. Analytical HPLC on an Agilent (1260) using C18 analytical column, H₂O/C₂H₅N (0.1%TFA) eluent at 1 mL/min flow, monitored by UV absorption at 254 nm, showed 94.6% purity.

5.9.6. (S,E)-N-(4-((3-chloro-4-fluorophenyl)amino)-7-((tetrahydrofuran-3-yl)oxy)quinazolin-6-yl)-2-((1-(2-(4-methylpiperazin-1-yl)ethyl)-1H-pyrrol-2-yl)methylene)hydrazine carboxamide (**19f**)

Yellow solid; mp 145.3–146.6 °C; yield: 50.3%; ¹H NMR (400 MHz, DMSO-*d*₆) δ 10.79 (s, 1H), 9.84 (s, 1H), 8.95 (s, 1H), 8.69 (s, 1H), 8.51 (s, 1H), 8.11 (d, *J* = 4.4 Hz, 1H), 7.98 (s, 1H), 7.78 (s, 1H), 7.41 (t, *J* = 9.2 Hz, 1H), 7.30 (s, 1H), 7.02 (s, 1H), 6.52 (s, 1H), 6.10 (s, 1H), 5.39 (s, 1H), 4.30 (s, 2H), 3.99 (s, 2H), 3.94 (d, *J* = 7.2 Hz, 1H), 3.81 (s, 1H), 2.51 (s, 2H), 2.40 (d, *J* = 6.0 Hz, 1H), 2.32 (s, 4H), 2.12 (s, 1H), 1.32 (s, 4H), 1.25 (s, 3H); ESI-MS *m/z*: [M + H]⁺ 637.2.

5.9.7. (S,E)-N-(4-((3-chloro-4-fluorophenyl)amino)-7-((tetrahydrofuran-3-yl)oxy)quinazolin-6-yl)-2-((1-(3-morpholinopropyl)-1H-pyrrol-2-yl)methylene)hydrazinecarboxamide (**19g**)

Yellow solid; mp 161.3–162.6 °C; yield: 58.2%; ¹H NMR (400 MHz, DMSO-*d*₆) δ 10.79 (s, 1H), 9.85 (s, 1H), 9.00 (s, 1H), 8.72 (s, 1H), 8.50 (s, 1H), 8.09 (d, *J* = 4.4 Hz, 1H), 8.02 (s, 1H), 7.79 (s, 1H), 7.42 (t, *J* = 9.0 Hz, 1H), 7.31 (s, 1H), 7.00 (s, 1H), 6.55 (s, 1H), 6.12 (s, 1H), 5.41 (s, 1H), 4.23 (s, 2H), 3.99 (s, 2H), 3.94 (d, *J* = 7.8 Hz, 1H), 3.80 (s, 1H), 3.52 (s, 4H), 2.44 (s, 1H), 2.24 (s, 4H), 2.14 (s, 3H), 1.83 (s, 2H); ESI-MS *m/z*: [M + H]⁺ 638.2.

5.9.8. (S,E)-N-(4-((3-chloro-4-fluorophenyl)amino)-7-((tetrahydrofuran-3-yl)oxy)quinazolin-6-yl)-2-((1-(3-(dimethylamino)propyl)-1H-pyrrol-2-yl)methylene)hydrazine carboxamide (**19h**)

Yellow solid; mp 179.4–180.6 °C; yield: 62.3%; ¹H NMR (400 MHz, DMSO-*d*₆) δ 10.80 (s, 1H), 9.84 (s, 1H), 8.98 (s, 1H), 8.71 (s, 1H), 8.50 (s, 1H), 8.15–8.01 (m, 2H), 7.78 (d, *J* = 3.1 Hz, 1H), 7.41 (t, *J* = 9.1 Hz, 1H), 7.30 (s, 1H), 7.00 (s, 1H), 6.56 (s, 1H), 6.13 (s, 1H), 5.40 (s, 1H), 4.25 (s, 2H), 3.99 (s, 2H), 3.95 (d, *J* = 7.9 Hz, 1H), 3.80 (d, *J* = 5.3 Hz, 1H), 2.45–2.35 (m, 3H), 2.27 (s, 6H), 2.10 (d, *J* = 6.1 Hz, 1H), 1.88 (s, 2H); ESI-MS *m/z*: [M + H]⁺ 595.2.

5.9.9. (S,E)-N-(4-((3-chloro-4-fluorophenyl)amino)-7-((tetrahydrofuran-3-yl)oxy)quinazolin-6-yl)-2-((1-(3-(diethylamino)propyl)-1H-pyrrol-2-yl)methylene)hydrazine carboxamide (**19i**)

Yellow solid; mp 158.3–159.6 °C; yield: 65.5%; ¹H NMR (400 MHz, DMSO-*d*₆) δ 10.79 (s, 1H), 9.85 (s, 1H), 8.99 (s, 1H), 8.70 (s, 1H), 8.50 (s, 1H), 8.10 (s, 1H), 8.01 (s, 1H), 7.79 (s, 1H), 7.42 (t, *J* = 9.3 Hz, 1H), 7.31 (s, 1H), 7.00 (s, 1H), 6.55 (s, 1H), 6.12 (s, 1H), 5.40 (s, 1H), 4.20 (s, 2H), 3.98 (s, 2H), 3.93 (d, *J* = 8.5 Hz, 1H), 3.80 (s, 1H), 2.46–2.31 (m, 5H), 2.28 (s, 2H), 2.10 (s, 1H), 1.78 (s, 2H), 0.84 (t, *J* = 6.8 Hz, 6H); ESI-MS *m/z*: [M + H]⁺ 624.2. ¹³C NMR (101 MHz, DMSO-*d*₆) δ 157.17, 153.55, 152.74, 151.51, 147.82, 137.44, 135.46, 128.86, 127.16, 126.80, 124.01, 122.95, 119.19, 116.92, 116.71, 113.22, 110.77, 109.97, 108.84, 108.41, 79.49, 72.75, 67.01, 49.37, 46.45(2C), 46.19, 32.93, 28.90, 11.77(2C). Analytical HPLC on an Agilent (1260) using C18

analytical column, H₂O/C₂H₅N (0.1%TFA) eluent at 1 mL/min flow, monitored by UV absorption at 254 nm, showed 96.2% purity.

5.9.10. (S,E)-N-(4-((3-chloro-4-fluorophenyl)amino)-7-((tetrahydrofuran-3-yl)oxy)quinazolin-6-yl)-2-((1-(3-(piperidin-1-yl)propyl)-1H-pyrrol-2-yl)methylene)hydrazine carboxamide (**19j**)

Yellow solid; mp 144.3–145.5 °C; yield: 60.5%; ¹H NMR (400 MHz, DMSO-*d*₆) δ 10.76 (s, 1H), 9.83 (s, 1H), 8.99 (s, 1H), 8.70 (s, 1H), 8.50 (s, 1H), 8.09 (dd, *J* = 6.7, 2.4 Hz, 1H), 8.01 (s, 1H), 7.83–7.72 (m, 1H), 7.41 (t, *J* = 9.1 Hz, 1H), 7.31 (s, 1H), 6.98 (s, 1H), 6.55 (s, 1H), 6.12 (s, 1H), 5.40 (s, 1H), 4.21 (s, 2H), 3.99 (s, 2H), 3.94 (dd, *J* = 15.3, 7.4 Hz, 1H), 3.83–3.76 (m, 1H), 2.43 (dd, *J* = 13.5, 6.3 Hz, 1H), 2.21 (s, 4H), 2.11 (s, 3H), 1.87–1.76 (m, 2H), 1.44 (s, 4H), 1.30 (s, 2H); ESI-MS *m/z*: [M + H]⁺636.2.

5.9.11. (S,E)-N-(4-((3-chloro-4-fluorophenyl)amino)-7-((tetrahydrofuran-3-yl)oxy)quinazolin-6-yl)-2-((1-(3-(pyrrolidin-1-yl)propyl)-1H-pyrrol-2-yl)methylene)hydrazine carboxamide (**19k**)

Yellow solid; mp 136.5–137.8 °C; yield: 66.3%; ¹H NMR (400 MHz, DMSO-*d*₆) δ 10.79 (s, 1H), 9.85 (s, 1H), 8.99 (s, 1H), 8.50 (s, 1H), 8.10 (d, *J* = 6.8 Hz, 1H), 8.00 (s, 1H), 7.95 (s, 1H), 7.78 (d, *J* = 8.4 Hz, 1H), 7.42 (t, *J* = 9.1 Hz, 1H), 7.31 (s, 1H), 6.99 (s, 1H), 6.54 (s, 1H), 6.12 (s, 1H), 5.40 (s, 1H), 4.25 (d, *J* = 4.8 Hz, 2H), 3.99 (s, 2H), 3.95–3.89 (m, 1H), 3.85–3.77 (m, 1H), 2.46–2.37 (m, 1H), 2.30 (d, *J* = 11.7 Hz, 4H), 2.27 (t, *J* = 6.9 Hz, 2H), 2.13–2.03 (m, 1H), 1.87–1.76 (m, 2H), 1.59 (s, 4H); ESI-MS *m/z*: [M + H]⁺622.2.

5.9.12. (S,E)-N-(4-((3-chloro-4-fluorophenyl)amino)-7-((tetrahydrofuran-3-yl)oxy)quinazolin-6-yl)-2-((1-(3-(4-methylpiperazin-1-yl)propyl)-1H-pyrrol-2-yl)methylene)hydrazine carboxamide (**19l**)

Yellow solid; mp 178.1–179.8 °C; yield: 71.2%; ¹H NMR (400 MHz, DMSO-*d*₆) δ 10.80 (s, 1H), 9.86 (s, 1H), 9.00 (s, 1H), 8.70 (s, 1H), 8.50 (s, 1H), 8.09 (d, *J* = 6.8 Hz, 1H), 8.01 (s, 1H), 7.78 (d, *J* = 5.2 Hz, 1H), 7.42 (t, *J* = 9.1 Hz, 1H), 7.31 (s, 1H), 6.99 (s, 1H), 6.55 (s, 1H), 6.12 (s, 1H), 5.41 (s, 1H), 4.23 (s, 2H), 3.99 (s, 2H), 3.95–3.88 (m, 1H), 3.79 (d, *J* = 5.2 Hz, 1H), 2.47–2.25 (m, 9H), 2.11 (m, 6H), 1.84 (d, *J* = 6.2 Hz, 2H); ESI-MS *m/z*: [M + H]⁺651.2.

5.9.13. (E)-N-(4-((3-chloro-4-fluorophenyl)amino)-7-methoxyquinazolin-6-yl)-2-((1-(2-morpholinoethyl)-1H-pyrrol-2-yl)methylene)hydrazine carboxamide (**20a**)

White solid; mp 153.4–154.8 °C; yield: 72.4%; ¹H NMR (400 MHz, DMSO-*d*₆) δ 10.76 (d, *J* = 12.7 Hz, 1H), 9.83 (s, 1H), 8.91 (s, 1H), 8.79 (d, *J* = 11.4 Hz, 1H), 8.52 (d, *J* = 5.0 Hz, 1H), 8.11 (d, *J* = 7.1 Hz, 1H), 7.94 (s, 1H), 7.79 (s, 1H), 7.42 (t, *J* = 9.0 Hz, 1H), 7.32 (d, *J* = 5.7 Hz, 1H), 7.04 (s, 1H), 6.49 (s, 1H), 6.13 (d, *J* = 11.7 Hz, 1H), 4.46 (t, *J* = 5.8 Hz, 2H), 4.07 (s, 3H), 3.38 (d, *J* = 14.2 Hz, 4H), 2.61 (t, *J* = 6.3 Hz, 2H), 2.35 (s, 4H); ESI-MS *m/z*: [M + H]⁺567.2. Analytical HPLC on an Agilent (1260) using C18 analytical column, H₂O/C₂H₅N (0.1%TFA) eluent at 1 mL/min flow, monitored by UV absorption at 254 nm, showed 94.4% purity.

5.9.14. (E)-N-(4-((3-chloro-4-fluorophenyl)amino)-7-methoxyquinazolin-6-yl)-2-((1-(2-(dimethylamino)ethyl)-1H-pyrrol-2-yl)methylene)hydrazine carboxamide (**20b**)

White solid; mp 182.7–183.8 °C; yield: 73.1%; ¹H NMR (400 MHz, DMSO-*d*₆) δ 10.75 (s, 1H), 9.82 (s, 1H), 8.91 (s, 1H), 8.83 (s, 1H), 8.51 (s, 1H), 8.10 (dd, *J* = 6.8, 2.5 Hz, 1H), 7.93 (d, *J* = 13.2 Hz, 1H), 7.83–7.73 (m, 1H), 7.41 (t, *J* = 9.1 Hz, 1H), 7.31 (s, 1H), 7.03 (s, 1H), 6.50–6.46 (m, 1H), 6.14–6.04 (m, 1H), 4.41 (t, *J* = 6.3 Hz, 2H), 4.06 (s, 3H), 2.56 (t, *J* = 6.5 Hz, 2H), 2.12 (s, 6H); ESI-MS *m/z*: [M + H]⁺525.1. ¹³C NMR (101 MHz, DMSO-*d*₆) δ 157.17, 154.12, 153.61, 152.96, 148.28, 137.44, 135.74, 128.51, 128.35, 126.42, 123.99, 122.93, 119.18, 116.92, 116.71, 115.86, 111.24, 109.83, 108.65, 106.87, 60.11, 56.94, 46.84, 45.80(2C). Analytical HPLC on an Agilent (1260) using

C18 analytical column, H₂O/C₂H₅N (0.1%TFA) eluent at 1 mL/min flow, monitored by UV absorption at 254 nm, showed 96.3% purity.

5.9.15. (E)-N-(4-((3-chloro-4-fluorophenyl)amino)-7-methoxyquinazolin-6-yl)-2-((1-(2-(diethylamino)ethyl)-1H-pyrrol-2-yl)methylene)hydrazinecarboxamide (**21c**)

White solid; mp 186.3–187.8 °C; yield: 75.3%; ¹H NMR (400 MHz, DMSO-*d*₆) δ 10.79 (s, 1H), 9.84 (s, 1H), 8.94 (s, 1H), 8.81 (s, 1H), 8.51 (s, 1H), 8.10 (s, 1H), 7.94 (s, 1H), 7.79 (s, 1H), 7.41 (s, 1H), 7.31 (s, 1H), 7.02 (s, 1H), 6.48 (s, 1H), 6.10 (s, 1H), 4.39 (s, 2H), 4.07 (s, 3H), 2.66 (s, 2H), 2.42 (s, 4H), 0.81 (s, 6H); ESI-MS *m/z*: [M + H]⁺553.2.

5.9.16. (E)-N-(4-((3-chloro-4-fluorophenyl)amino)-7-methoxyquinazolin-6-yl)-2-((1-(2-(piperidin-1-yl)ethyl)-1H-pyrrol-2-yl)methylene)hydrazine carboxamide (**20d**)

White solid; mp 165.3–167.5 °C; yield: 70.2%; ¹H NMR (400 MHz, DMSO-*d*₆) δ 10.79 (s, 1H), 9.84 (s, 1H), 8.92 (s, 1H), 8.77 (d, *J* = 16.7 Hz, 1H), 8.51 (s, 1H), 8.10 (dd, *J* = 6.8, 2.5 Hz, 1H), 7.93 (s, 1H), 7.78 (dd, *J* = 7.2, 4.6 Hz, 1H), 7.42 (t, *J* = 9.1 Hz, 1H), 7.30 (d, *J* = 12.5 Hz, 1H), 7.01 (d, *J* = 8.7 Hz, 1H), 6.48 (d, *J* = 2.1 Hz, 1H), 6.14–6.05 (m, 1H), 4.43 (t, *J* = 6.5 Hz, 2H), 4.07 (s, 4H), 2.56 (d, *J* = 6.6 Hz, 2H), 2.32 (s, 4H), 1.38 (m, 6H); ESI-MS *m/z*: [M + H]⁺565.2. Analytical HPLC on an Agilent (1260) using C18 analytical column, H₂O/C₂H₅N (0.1%TFA) eluent at 1 mL/min flow, monitored by UV absorption at 254 nm, showed 96.9% purity.

5.9.17. (E)-N-(4-((3-chloro-4-fluorophenyl)amino)-7-methoxyquinazolin-6-yl)-2-((1-(2-(pyrrolidin-1-yl)ethyl)-1H-pyrrol-2-yl)methylene)hydrazine carboxamide (**20e**)

White solid; mp 145.2–146.5 °C; yield: 68.3%; ¹H NMR (400 MHz, DMSO-*d*₆) δ 10.80 (s, 1H), 9.84 (s, 1H), 8.85 (d, *J* = 19.0 Hz, 2H), 8.51 (s, 1H), 8.12 (s, 1H), 7.94 (s, 1H), 7.80 (s, 1H), 7.53–7.36 (m, 1H), 7.30 (s, 1H), 7.03 (s, 1H), 6.48 (s, 1H), 6.10 (s, 1H), 4.43 (s, 2H), 4.05 (s, 3H), 2.73 (s, 2H), 2.40 (m, 4H), 1.48 (m, 4H); ESI-MS *m/z*: [M + H]⁺551.2.

5.9.18. (E)-N-(4-((3-chloro-4-fluorophenyl)amino)-7-methoxyquinazolin-6-yl)-2-((1-(2-(4-methylpiperazin-1-yl)ethyl)-1H-pyrrol-2-yl)methylene)hydrazine carboxamide (**20f**)

White solid; mp 185.3–186.5 °C; yield: 63.4%; ¹H NMR (400 MHz, DMSO-*d*₆) δ 10.79 (s, 1H), 9.83 (s, 1H), 8.92 (s, 1H), 8.80 (s, 1H), 8.51 (s, 1H), 8.10 (dd, *J* = 6.8, 2.4 Hz, 1H), 7.94 (s, 1H), 7.85–7.74 (m, 1H), 7.41 (t, *J* = 9.1 Hz, 1H), 7.30 (d, *J* = 11.0 Hz, 1H), 7.02 (s, 1H), 6.48 (s, 1H), 6.11 (d, *J* = 2.8 Hz, 1H), 4.44 (d, *J* = 6.3 Hz, 2H), 4.07 (s, 3H), 2.55 (d, *J* = 8.1 Hz, 2H), 2.33 (s, 3H), 1.27 (m, 8H); ESI-MS *m/z*: [M + H]⁺580.2.

5.9.19. (E)-N-(4-((3-chloro-4-fluorophenyl)amino)-7-methoxyquinazolin-6-yl)-2-((1-(3-morpholinopropyl)-1H-pyrrol-2-yl)methylene)hydrazine carboxamide (**20g**)

White solid; mp 178.1–179.3 °C; yield: 75.4%; ¹H NMR (400 MHz, DMSO-*d*₆) δ 10.77 (s, 1H), 9.83 (s, 1H), 8.96 (s, 1H), 8.80 (s, 1H), 8.50 (s, 1H), 8.08 (dd, *J* = 6.7, 2.3 Hz, 1H), 7.95 (s, 1H), 7.78 (dd, *J* = 8.2, 3.4 Hz, 1H), 7.39 (dd, *J* = 19.9, 10.8 Hz, 1H), 7.32 (s, 1H), 7.01 (s, 1H), 6.50 (s, 1H), 6.12 (d, *J* = 2.7 Hz, 1H), 4.38 (t, *J* = 6.1 Hz, 2H), 4.06 (s, 3H), 3.51 (d, *J* = 3.8 Hz, 4H), 2.24 (s, 4H), 2.16 (t, *J* = 6.7 Hz, 2H), 1.94–1.84 (m, 2H); ESI-MS *m/z*: [M + H]⁺582.2.

5.9.20. (E)-N-(4-((3-chloro-4-fluorophenyl)amino)-7-methoxyquinazolin-6-yl)-2-((1-(3-(dimethylamino)propyl)-1H-pyrrol-2-yl)methylene)hydrazine carboxamide (**20h**)

White solid; mp 189.5–190.8 °C; yield: 72.5%; ¹H NMR (400 MHz, DMSO-*d*₆) δ 10.80 (s, 1H), 9.85 (s, 1H), 8.96 (s, 1H), 8.80 (s, 1H), 8.51 (s, 1H), 8.10 (s, 1H), 7.95 (s, 1H), 7.79 (s, 1H), 7.51–7.38 (m, 1H), 7.32 (s, 1H), 7.00 (s, 1H), 6.49 (s, 1H), 6.12 (s, 1H), 4.37 (s, 2H), 4.07 (s, 3H), 2.07 (d, *J* = 31.7 Hz, 8H), 1.83 (s, 2H); ESI-MS *m/z*: [M + H]⁺ 539.2.

5.9.21. (*E*)-*N*-4-((3-chloro-4-fluorophenyl)amino)-7-methoxyquinazolin-6-yl)-2-((1-(3-(diethylamino)propyl)-1*H*-pyrrol-2-yl)methylene)hydrazine carboxamide (**20i**)

White solid; mp 190.3–191.4 °C; yield: 70.2%; ¹H NMR (400 MHz, DMSO-*d*₆) δ 10.80 (s, 1H), 9.84 (s, 1H), 8.96 (s, 1H), 8.78 (s, 1H), 8.50 (s, 1H), 8.10 (s, 1H), 7.94 (s, 1H), 7.79 (s, 1H), 7.37 (d, *J* = 16.7 Hz, 2H), 7.00 (s, 1H), 6.50 (s, 1H), 6.12 (s, 1H), 4.36 (s, 2H), 4.06 (s, 3H), 2.36 (d, *J* = 7.1 Hz, 6H), 1.84 (s, 2H), 0.83 (d, *J* = 6.6 Hz, 6H); ESI-MS *m/z*: [M + H]⁺567.2.

5.9.22. (*E*)-*N*-4-((3-chloro-4-fluorophenyl)amino)-7-methoxyquinazolin-6-yl)-2-((1-(3-(piperidin-1-yl)propyl)-1*H*-pyrrol-2-yl)methylene)hydrazine carboxamide (**20g**)

White solid; mp 175.3–176.8 °C; yield: 65.3%; ¹H NMR (400 MHz, DMSO-*d*₆) δ 10.80 (s, 1H), 9.85 (s, 1H), 8.95 (d, *J* = 14.7 Hz, 1H), 8.79 (s, 1H), 8.51 (s, 1H), 8.14–8.05 (m, 1H), 7.94 (s, 1H), 7.84–7.73 (m, 1H), 7.42 (t, *J* = 9.1 Hz, 1H), 7.32 (s, 1H), 6.99 (s, 1H), 6.49 (s, 1H), 6.11 (s, 1H), 4.36 (s, 2H), 4.06 (s, 3H), 2.20 (s, 4H), 2.12 (t, *J* = 6.9 Hz, 2H), 1.91–1.82 (m, 2H), 1.42 (d, *J* = 5.2 Hz, 4H), 1.30 (s, 2H); ESI-MS *m/z*: [M + H]⁺579.2. Analytical HPLC on an Agilent (1260) using C18 analytical column, H₂O/C₂H₅N (0.1%TFA) eluent at 1 mL/min flow, monitored by UV absorption at 254 nm, showed 97.1% purity.

5.9.23. (*E*)-*N*-4-((3-chloro-4-fluorophenyl)amino)-7-methoxyquinazolin-6-yl)-2-((1-(3-(pyrrolidin-1-yl)propyl)-1*H*-pyrrol-2-yl)methylene)hydrazine carboxamide (**20k**)

White solid; mp 185.5–186.8 °C; yield: 68.2%; ¹H NMR (400 MHz, DMSO-*d*₆) δ 10.80 (s, 1H), 9.85 (s, 1H), 8.97 (s, 1H), 8.81 (s, 1H), 8.50 (s, 1H), 8.09 (d, *J* = 4.6 Hz, 1H), 7.94 (s, 1H), 7.79 (s, 1H), 7.41 (t, *J* = 9.1 Hz, 1H), 7.32 (s, 1H), 7.00 (s, 1H), 6.49 (s, 1H), 6.11 (s, 1H), 4.39 (d, *J* = 5.9 Hz, 2H), 4.06 (s, 3H), 2.39–2.23 (m, 6H), 1.92–1.82 (m, 2H), 1.58 (s, 4H); ESI-MS *m/z*: [M + H]⁺565.2.

5.9.24. (*E*)-*N*-4-((3-chloro-4-fluorophenyl)amino)-7-methoxyquinazolin-6-yl)-2-((1-(3-(4-methylpiperazin-1-yl)propyl)-1*H*-pyrrol-2-yl)methylene)hydrazine carboxamide (**20l**)

White solid; mp 165.5–166.8 °C; yield: 63.4%; ¹H NMR (400 MHz, DMSO-*d*₆) δ 10.78 (s, 1H), 9.84 (s, 1H), 8.97 (s, 1H), 8.79 (s, 1H), 8.50 (s, 1H), 8.09 (dd, *J* = 6.8, 2.5 Hz, 1H), 7.94 (s, 1H), 7.79 (dd, *J* = 9.0, 2.7 Hz, 1H), 7.41 (t, *J* = 9.1 Hz, 1H), 7.32 (s, 1H), 7.00 (s, 1H), 6.49 (d, *J* = 2.1 Hz, 1H), 6.17–6.04 (m, 1H), 4.38 (d, *J* = 6.3 Hz, 2H), 4.06 (s, 3H), 2.18 (m, 15.7 Hz, 10H), 2.05 (s, 3H), 1.91–1.79 (m, 2H); ESI-MS *m/z*: [M + H]⁺594.2.

5.10. Cytotoxicity assay in vitro

The cytotoxic activities of target compounds (**10a–e**, **11a–e**, **14a–f**, **15a–f**, **19a–l** and **20a–l**) were evaluated with A549, HepG2, MCF-7 or/and PC-3 cell lines by the standard MTT assay in vitro, with EGFR inhibitors Afatinib as positive control. The cancer cell lines were cultured in minimum essential medium (MEM) supplement with 10% fetal bovine serum (FBS). Approximately 4 × 10³ cells, suspended in MEM medium, were plated onto each well of a 96-well plate and incubated in 5% CO₂ at 37 °C for 24 h. The tested compounds at indicated final concentrations were added to the culture medium and the cell cultures were continued for 72 h. Fresh MTT was added to each well at a terminal concentration of 5 µg/mL and incubated with cells at 37 °C for 4 h. The formazan crystals were dissolved in 100 µL DMSO each well, and the absorbency at 492 nm (for absorbance of MTT formazan) and 630 nm (for the reference wavelength) was measured with the ELISA reader. All of the compounds were tested three times in each of the cell lines. The results expressed as inhibition rates or IC₅₀ (half-maximal inhibitory concentration) were the averages of two determinations and calculated by using the Bacus Laboratories Incorporated Slide Scanner (Bliss) software.

5.11. EGFR kinases assay in vitro

The target compounds (**14a**, **14b**, **14c**, **14d**, **14f**, **19a**, **19b**, **19i**, **19j**, **20b**, and **20h**) were tested for their activity against EGFR kinases through the mobility shift assay. All kinases assays were performed in 96-well plates in a 50 µL reaction volume. The kinase buffer contains 50 mM HEPES, pH 7.5, 10 mM MgCl₂, 0.0015% Brij-35 and 2 mM DTT. The stop buffer contains 100 mM HEPES, pH 7.5, 0.015% Brij-35, 0.2% Coating Reagent #3 and 50 mM EDTA. Dilute the compounds to 500 µM by 100% DMSO, then transfer 10 µL of compound to a new 96-well plate as the intermediate plate, add 90 µL kinase buffer to each well. Transfer 5 µL of each well of the intermediate plate to 384-well plates. The following amounts of enzyme and substrate were used per well: kinase base buffer, FAM-labeled peptide, ATP and enzyme solution. Wells containing the substrate, enzyme, DMSO without compound were used as DMSO control. Wells containing just the substrate without enzyme were used as low control. Incubate at room temperature for 10 min. Add 10 µL peptide solution to each well. Incubate at 28 °C for specified period of time and stop reaction by 25 µL stop buffer. At last collect data on Caliper program and convert conversion values to inhibition values. Percent inhibition = (max – conversion)/(max – min) × 100. “max” stands for DMSO control; “min” stands for low control.

5.12. Observation of nuclear morphology

The cancer cell lines were cultured in minimum essential medium (MEM) supplement with 10% fetal bovine serum (FBS). Approximately 2 × 10⁴ cells, suspended in MEM medium, were plated onto each well of a 24-well plate and incubated in 5% CO₂ at 37 °C for 24 h. Then the medium was removed, and 1 mL drug-free medium and 1 mL medium with the tested compounds (**14d** and **19b**) at indicated final concentrations were added to each well in control group and tested group respectively and the cell cultures were continued for 12 h. While the medium was removed, AO-PBS buffer was added to each well at a terminal concentration of 10 µg/mL and stained in dark for 10 min. Each well was washed with PBS buffer three times and observed under a fluorescence microscope.

5.13. Cell cycle analysis

A549 cells were seeded in 16-well plates at a density of 1 × 10⁶ cells/well in DMEM, then treated with 1 time concentration of Afatinib, **14b**, **19b** and treated without compounds for 12 h, respectively. Cultured cells were stained with PerCP in the dark at 4 °C for 30 min and analyzed by ACEA NovoCyte™.

5.14. Docking studies

For docking purposes, the three-dimensional structure of the EGFR (PDB code: 4G5P) was obtained from RCSB Protein Data Bank [16]. Hydrogen atoms were added to the structure allowing for appropriate ionization at physiological pH. The protonated state of several important residue were adjusted by using SYBYL6.9.1 (Tripos, St. Louis, USA) in favor of forming reasonable hydrogen bond with the ligand. Molecular docking analysis was carried out by the SURFLEX-DOCK module of SYBYL 6.9.1 package to explore the binding model for the active site of c-Met with its ligand. All atoms located within the range of 5.0 Å from any atom of the cofactor were selected into the active site, and the corresponding amino acid residue was, therefore, involved into the active site if only one of its atoms was selected. Other default parameters were adopted in the SURFLEX-DOCK calculations. All calculations were performed on Silicon Graphics workstation.

Acknowledgments

We gratefully acknowledge the generous support provided by The National Natural Science Funds of China (No. 21662014), Outstanding Youth Foundation of Jiangxi, Natural Science Foundation of Jiangxi, China (20171BCB23078), Natural Science Foundation of Jiangxi, China (20171ACB21052 & 20171BAB215073), Natural Science Foundation of Jiangxi, China (20171BAB205101), Innovative Research Team of Jiangxi Science & Technology Normal University (2017CXTD002).

Conflict of interest

The authors have no conflict of interest.

Appendix A. Supplementary data

Supplementary data to this article can be found online at <https://doi.org/10.1016/j.csbj.2018.10.016>.

References

- [1] Sharma SV, Bell DW, Settleman J, et al. Epidermal growth factor receptor mutations in lung cancer. *Nat Rev Cancer* 2007;7:169–81.
- [2] Cheng G, Park S, Shu S, et al. Advances of AKT pathway in human oncogenesis and as a target for anti-cancer drug discovery. *Curr Cancer Drug Targets* 2008;8:2–6.
- [3] Song Z, Ge Y, Wang C, et al. Challenges and perspectives on the development of small-molecule EGFR inhibitors against T790M-mediated resistance in non-small-cell lung cancer. *J Med Chem* 2016;59:6580–94.
- [4] Peraldoneia C, Migliardi G, Mellogrand M, et al. Epidermal growth factor receptor (EGFR) mutation analysis, gene expression profiling and EGFR protein expression in primary prostate cancer. *BMC Cancer* 2011;11:1–12.
- [5] Cohen MH, Williams GA, Sridhara R, et al. FDA drug approval summary: gefitinib (ZD1839) (iressa) tablets. *Oncologist* 2003;8:303–6.
- [6] Fukuoka M, Yano S, Giaccone G, et al. Multi-institutionalran- domized phase II trial of gefitinib for previously treated patients with advanced non-small-cell lung cancer. *J Clin Oncol* 2003;23:2237–46.
- [7] Carmi C, Mor M, Petronini PG, et al. Clinical perspectives for irreversible tyrosine kinase inhibitors in cancer. *Biochem Pharmacol* 2012;84:1388–99.
- [8] Beau FM, Ruppert AM, Voegeli AC, et al. MET gene copy number in non-small cell lung cancer: molecular analysis in a targeted tyrosine kinase inhibitor naive cohort. *J Thorac Oncol* 2008;3:331–9.
- [9] Chen X, Zhu Q, Zhu L, et al. Clinical perspective afatinib in non-small cell lung cancer. *Lung Cancer* 2013;81:155–61.
- [10] Y Tu, Wang C, S Xu, et al. Design, synthesis, and docking studies of quinazoline analogues bearing aryl semicarbazone scaffolds as potent EGFR inhibitors. *Bioorg Med Chem* 2017;25:3148–57.
- [11] Gefitinib VJ. (Iressa, ZD1839): a novel targeted approach for the treatment of solid tumors. *Bull Cancer* 2004;91:10070–6.
- [12] US Fda. FDA Approves New Treatment for a Type of Late-Stage Lung Cancer [EB/OL. [2013-07-12]] <http://www.Fda.gov/NewsEvents/Newsroom/PressAnnouncements/ucm360499.htm>
- [13] Ramalingam SS, Yang James C, et al. AZD9291, a mutant-selective EGFR inhibitor, as first-line treatment for EGFR mutation-positive advanced non-small cell lung cancer (NSCLC): results from a phase 1 expansion cohort. *J Clin Oncol* 2015;33(15-Suppl): 8000.
- [14] Eberlein C, Stetson D, Markovets A, et al. Acquired resistance to mutant-selective EGFR inhibitor AZD9291 is associated with increased dependence on RAS signaling in preclinical models. *Cancer Res* 2015;75:2489–500.
- [15] Thress KS, Paweletz CP, Felip E, et al. Acquired EGFR C797S mutation mediates resistance to AZD9291 in non-small cell lung cancer harboring EGFR T790M. *Nature Med* 2015;21:560–2.
- [16] Bryan MC, Burdick DJ, Chan BK, et al. Pyridones as highly selective, noncovalent inhibitors of T790M double mutants of EGFR. *ACS Med Chem Lett* 2016;7:100–4.
- [17] Heald R, Bowman KK, Bryan MC, et al. Noncovalent mutant selective epidermal growth factor receptor inhibitors: a lead optimization case study. *J Med Chem* 2015;58:8877–95.
- [18] Qin M, Zhai X, Xie H, et al. Design and synthesis of novel 2-(4-(2-(dimethylamino) ethyl)-4H-1,2,4-triazol-3-yl)pyridines as potential antitumor agents. *Eur J Med Chem* 2014;81:47–58.
- [19] Zhai X, Bao G, Wang L, et al. Design, synthesis and biological evaluation of novel 4-phenoxy-6,7-disubstituted quinolines possessing (thio)semicarbazones as c-Met kinase inhibitors. *Bioorg Med Chem* 2016;24:1331–45.
- [20] Y Tu, Ouyang Y, S Xu, et al. Design, synthesis, and docking studies of afatinib analogs bearing cinnamamide moiety as potent EGFR inhibitors. *Bioorg Med Chem* 2016;24: 1495–503.
- [21] Chen C, Bocian DF, Lindsey JS. Synthesis of 24 bacteriochlorin isotopologues, each containing a symmetrical pair of ¹³C or ¹⁵N atoms in the inner core of the macrocycle. *J Org Chem* 2014;79:1001–16.
- [22] Solca F, Dahl G, Zoepfel A, et al. Crystal structure of EGFR kinase in complex with BIBW2992. *J Pharmacol Exp Ther* 2012;343:342–50.
- [23] Close A, Jones R, Ocasio C, et al. Elaboration of tetra-orthogonally-substituted aromatic scaffolds towards novel EGFR-kinase inhibitors. *Org Biomol Chem* 2016;14: 8246–52.